arXiv:1406.6649v2 [hep-ph] 21 Sep 2014

The perturbative QCD factorization of $\rho\gamma^\star \to \pi$

Shan Cheng[1*] and Zhen-Jun Xiao[1,2†]

1. Department of Physics and Institute of Theoretical Physics, Nanjing Normal University, Nanjing, Jiangsu 210023, People's Republic of China, and

2. Jiangsu Key Laboratory for Numerical Simulation of Large Scale Complex Systems, Nanjing Normal University, Nanjing 210023, People's Republic of China

(Dated: September 23, 2014)

In this paper, we firstly varify that the factorization hypothesis is valid for the exclusive process $\rho\gamma^\star \to \pi$ at the next-to-leading order (NLO) with the collinear factorization approach, and then extend this proof to the case of the k_T factorization approach. We particularly show that at the NLO level, the soft divergences in the full quark level calculation could be canceled completely as for the $\pi\gamma^\star \to \pi$ process where only the pseudoscalar π meson involved, and the remaining collinear divergences can be absorbed into the NLO hadron wave functions. The full amplitudes can be factorized as the convolution of the NLO wave functions and the infrared-finite hard kernels with these factorization approaches. We also write out the NLO meson distribution amplitudes in the form of nonlocal matrix elements.

PACS numbers: 11.80.Fv, 12.38.Bx, 12.38.Cy, 12.39.St

I. INTRODUCTION

As the fundamental tool of the perturbative Quantum Chromodynamics(QCD)[1] with a large momentum translation, the factorization theorem [2] assume that the hard part of the relevant processes is infrared-finite and can be calculated, while the non-perturbative dynamics of these high-energy QCD processes can be canceled at the quark level or absorbed into the input universal hadron wave functions. The physical quantities can be written as the convolutions of the hard part kernels and the universal processes-independent wave functions, and then the perturbative QCD has the prediction power. The collinear factorization [3, 4] and the k_T factorization [5–7], with the distinction whether to keep the transversal momenta in the propergators, are the two popular factorization approaches applied on the kard QCD processes.

We know that the theoretical study for the exclusive processes are in general more difficult than that for the inclusive processes [8]. Because in the exclusive processes, the pQCD factorization in it's standard form may be valid only for the large momentum transfer processes; while in the inclusive processes, like the deep-inelastic scattering, the leading twist factorization approximation is adequate already at $Q \sim 1$ Gev. So the intensively investigation for the factorization theorems or the factorization approaches for the exclusive processes is unavoidable.

In recent years, based on the factorization hypothesis, the collinear factorization and k_T factorization for the exclusive processes $\pi\gamma^\star \to \gamma(\pi)$ and $B \to \gamma(\pi)l\overline{\nu}$ have been testified both at the leading order (LO) and the next-to-leading order (NLO) level, and then these factorization

* chengshan-anhui@163.com
† xiaozhenjun@njnu.edu.cn

proofs were developed into all-orders with the induction approach[9–11]. The NLO hard kernels for these exclusive processes have also been calculated for example in Refs. [12–16]. These NLO evaluations showed that the positive corrections from the leading twist would be cancelled partly by the negative corrections from the NLO twist, resulting in a small net NLO correction to the leading order hard kernels, which further verified the feasibility of the perturbative QCD to those considered exclusive processes. But all these proofs and calculations are only relevant for the pseudo-scalar mesons, the exclusive processes with vector mesons have not been included at present. The study of the electromagnetic form factor processes between the vector meson and the pseudo-scalar meson is an important way to understand the internal structure of hadrons. There are many works on this subject: (a) ρ meson transition and electromagnetic form factors are predicted at the NLO level in the QCD sum rule analysis[17]; (b) space-like and time-like pion-rho transition form factors were investigated in Ref. [18] in the light-cone formalism; (c) the meson transition form factors were studied within a model of QCD based on the Dyson-Schwinger equations in[19]; and (d) the transition form factor of $\rho\gamma^\star \to \pi$ was also extracted from the other processes in the extended hard-wall AdS/QCD model[20] recently.

In this paper, we also consider the rho-pion transition process. By inserting the Fierz identity into the relevant expressions and employing the eikonal approximation, we can factorize the fermion flow and the momentum flow effectively. By summing over all the color factors, we can express these irreducible convolutions into three parts: with the additional gluon momentum flow, not flow and partly flow into the leading order hard kernel. We will do the factorization proof for the exclusive process $\rho\gamma^\star \to \pi$ at the NLO level, from the collinear factorization to the k_T factorization approach. With the light-cone kinetics, we will obtain the gauge invariant nonlocal matrix element for the pion meson and rho meson wave functions along the light-cone direction in the collinear factorization, and lightly deviate from the light-cone direction in the k_T factorization. At the NLO level, we clearly verified that the soft divergences will be canceled in the quark level diagrams, and the collinear divergences can be absorbed into the NLO wave functions, then we can obtain an infrared-finite next-to-leading order hard kernel in principle.

The paper is organized as following. The leading order dynamical analysis is presented in the second section. In section-III we prove that the collinear factorization approach is valid for the $\rho \to \pi$ transition process at the next-to-leading order. The collinear factorization approach is extended to the k_T factorization approach for this $\rho \to \pi$ transition process in section-VI. The summary and some discussions will appear at the final section.

II. COLLINEAR FACTORIZATION OF $\rho\gamma^\star \to \pi$

In this section we will prove the collinear factorization of the transition $\rho\gamma^\star \to \pi$. We firstly consider the two sets of leading order transition amplitudes, and then use the Fierz identity and the eikonal approximation to factorize the fermion currents and the momentum currents at the NLO level, in order to obtain the NLO transition amplitudes for each sub-diagram in the convoluted forms of the LO hard transition amplitudes and the gauge invariant nonlocal NLO distribution amplitudes(DAs) along the light-core(LC) direction. We finally sum up all the sub-diagrams for each set to collect all the color factors. The key point of the factorization is to find and absorb the infrared divergences, so we will not consider the self-energy corrections to the internal quark lines because they don't generate infrared divergences.

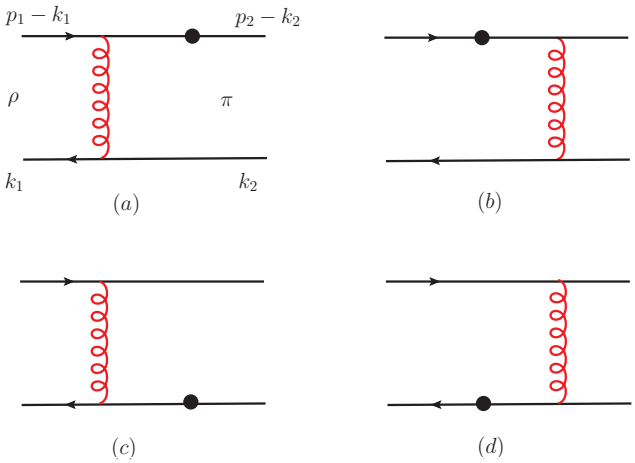

FIG. 1. The four leading-order quark diagrams for the $\rho\gamma^\star \to \pi$ form factor with the symbol $\bullet$ representing the virtual photon vertex.

A. Leading Order Hard Kernel

The LO quark diagrams for the $\rho\gamma^\star \to \pi$ transition are shown in the Fig. 1, where the virtual photon vertex represented by the dark spot have been placed at the four different positions respectively. In the light-cone coordinator system, the incoming ρ meson carry the momenta $p_1 = \frac{Q}{\sqrt{2}}(1, 0, \mathbf{0_T})$, and the outgoing π carry the momenta $p_2 = \frac{Q}{\sqrt{2}}(0, 1, \mathbf{0_T})$. Besides the momenta, the initial ρ would carry the longitudinal polarization vector $\epsilon_{1\mu}(L) = \frac{1}{\sqrt{2}\gamma_\rho}(1, -\gamma_\rho, \mathbf{0_T})$ and the transversal polarization vector $\epsilon_{1\mu}(T) = (0, 0, \mathbf{1_T})$. The momenta carried by the anti-quark of the initial and final state meson are defined as $k_1 = \frac{Q}{\sqrt{2}}(x_1, 0, \mathbf{0_T})$ and $k_2 = \frac{Q}{\sqrt{2}}(0, x_2, \mathbf{0_T})$ with x_1 and x_2 being the momentum fraction carried by the anti-partons inside ρ and π.

As the spin-1 particle, the wave functions for ρ meson should contain both longitudinal and transverse components[21].

$$\Phi_\rho(p_1, \epsilon_{1T}) = \frac{i}{\sqrt{2N_c}}\left[M_\rho \not{\epsilon}_{1T}\phi_\rho^v(x_1) + \not{\epsilon}_{1T}\not{p}_1\phi_\rho^T(x_1) + M_\rho i\epsilon_{\mu'\nu\rho\sigma}\gamma_5\gamma^{\mu'}\epsilon_{1T}^\nu n^\rho v^\sigma \phi_\rho^a(x_1)\right],$$
$$\Phi_\rho(p_1, \epsilon_{1L}) = \frac{i}{\sqrt{2N_c}}\left[M_\rho \not{\epsilon}_{1L}\phi_\rho(x_1) + \not{\epsilon}_{1L}\not{p}_1\phi_\rho^t(x_1) + M_\rho\phi_\rho^s(x_1)\right], \quad (1)$$

in which ϕ_ρ and ϕ_ρ^T are twist-2 (T2) DAs, $\phi_\rho^{t/s}$, $\phi_\rho^{t/s}$ are twist-3 (T3) DAs, and the unit vector n/v is defined as $(1, 0, \mathbf{0})/(0, 1, \mathbf{0})$. The pseudoscalar π meson wave function up to twist-3 is also given as in Refs. [22–24]

$$\Phi_\pi(p_2) = \frac{-i}{\sqrt{2N_c}}\left\{\gamma_5\not{p}_2\phi_\pi^a(x_2) + m_0^\pi\gamma_5\left[\phi_\pi^p(x_2) + (\not{v}\not{n} - 1)\phi_\pi^t(x_2)\right]\right\}, \quad (2)$$

with the twist-2 DA ϕ_π^a and twist-3 DAs ϕ_π^p and ϕ_π^t. The operator product expansion (OPE)[25] states that amplitudes from the twist-3 DAs are suppressed by the hierarchy M_ρ/Q and m_0^π/Q at the large momenta transition region, when compared with the twist-2 DAs of the ρ and π meson wave functions respectively. We can classify the LO transition amplitudes into four sets by the

twists' analysis of the initial and final meson wave functions: T2&T2; T2&T3; T3&T2 and finally T3&T3. Fortunately, we just need to consider the first two sub-diagrams Fig. 1(a) and Fig. 1(b) directly, because the amplitudes of sub-diagram Fig. 1(c) (Fig. 1(d)) can be obtained by simple replacement $x_i \to 1 - x_i (i = 1, 2)$ from the amplitudes of Fig. 1(a) (Fig. 1(b)). The standard calculations show that only the T3&T2 set (the twist-3 DAs of the rho meson and the twist-2 DAs of the pion meson) contribute to the LO transition amplitude of Fig. 1(a), which can be written as the following form,

$$G^{(0)}_{a,32}(x_1, x_2) = \frac{ieg_s^2 C_F}{2} \frac{[\not\epsilon_{1T} M_\rho \phi^v_\rho + M_\rho i\epsilon_{\mu'\nu\rho\sigma}\gamma_5\gamma^{\mu'}\epsilon^\nu_{1T} n^\rho v^\sigma \phi^a_\rho]\gamma^\alpha[\gamma_5 \not p_2 \phi^A_\pi]\gamma_\mu(\not p_1 - \not k_2)\gamma_\alpha}{(p_1 - k_2)^2(k_1 - k_2)^2}, \quad (3)$$

where γ^α should be chosen as γ^-. Similarly, only the crossed sets of T2&T3 (Set-I) and T3&T2 (Set-II) contribute to the LO transition amplitudes of Fig. 1(b), which can be written as the form of

$$G^{(0)}_{b,23}(x_1, x_2) = \frac{ieg_s^2 C_F}{2} \frac{[\not\epsilon_{1T} \not p_1 \phi^T_\rho]\gamma^\alpha[\gamma_5 m^0_\pi \phi^P_\pi]\gamma_\alpha(\not p_2 - \not k_1)\gamma_\mu}{(p_2 - k_1)^2(k_1 - k_2)^2}, \quad (4)$$

where the γ^α can be γ^- or $\gamma^\alpha_\perp$;

$$G^{(0)}_{b,32}(x_1, x_2) = \frac{ieg_s^2 C_F}{2} \frac{[\not\epsilon_{1T} M_\rho \phi^v_\rho + M_\rho i\epsilon_{\mu'\nu\rho\sigma}\gamma_5\gamma^{\mu'}\epsilon^\nu_{1T} n^\rho v^\sigma \phi^a_\rho]\gamma^\alpha[\gamma_5 \not p_2 \phi^A_\pi]\gamma_\alpha(\not p_2 - \not k_1)\gamma_\mu}{(p_2 - k_1)^2(k_1 - k_2)^2}, \quad (5)$$

where the $\gamma^\alpha = \gamma^\alpha_\perp$. The LO transition amplitudes as given in Eqs. (3,4,5) are all transversal due to the γ_5 from the final pion meson wave function, the γ_μ from the virtual photon vertex and the polarization vector ϵ_1 of the initial ρ meson.

From the expressions of the LO transition amplitudes $G^{(0)}(x_1, x_2)$ as given in Eqs. (3,4,5), one can see that there are clear qualitative differences between the $\rho\gamma^\star \to \pi$ studied in this paper and the $\pi\gamma^\star \to \pi$ investigated previously in Refs. [9, 11, 13, 15]:

(i) In the $\pi\gamma^\star \to \pi$ transition, the initial and final state meson are the same pion. Consequently, only the contribution from Fig. 1(a) should be calculated explicitly, while the contributions from Figs. 1(b,c,d) can be obtained from those of Fig. 1(a) by direct kinetic transformations [13, 15]. Furthermore, only the T2&T2 and T3&T3 terms contribute to the LO transition amplitudes because of the presence of matrix γ_5 in both the initial and final state pion meson.

(ii) For $\rho\gamma^\star \to \pi$ transition, however, the initial and final state meson are the vector ρ and pseudo-scalar pion. The possible contributions from Figs. 1(a) and 1(b) are rather different and should be calculated explicitly. For $\rho\gamma^\star \to \pi$ transition, in fact, only the transversal component $\Phi_\rho(p_1, \epsilon_{1T})$ of initial rho meson in Eq. (1) contribute to the LO rho-pion transition amplitude, and this LO transition amplitude receive the contributions from $G^{(0)}_{a,32}(x_1, x_2)$ in Eq. (3)(i.e. the crossed-set T3&T2) from Fig. 1(a), and from $G^{(0)}_{b,23}(x_1, x_2)$ and $G^{(0)}_{b,32}(x_1, x_2)$ in Eqs. (4,5)(i.e. the crossed sets T2&T3 and T3&T2) from Fig. 1(b).

B. $\mathcal{O}(\alpha_s)$ corrections to Fig.1(a)

A complete amplitude for a physical process in QCD is usually defined in three spaces: the spin space, the momenta space and the color space. So the factorization theorems need to deal with all

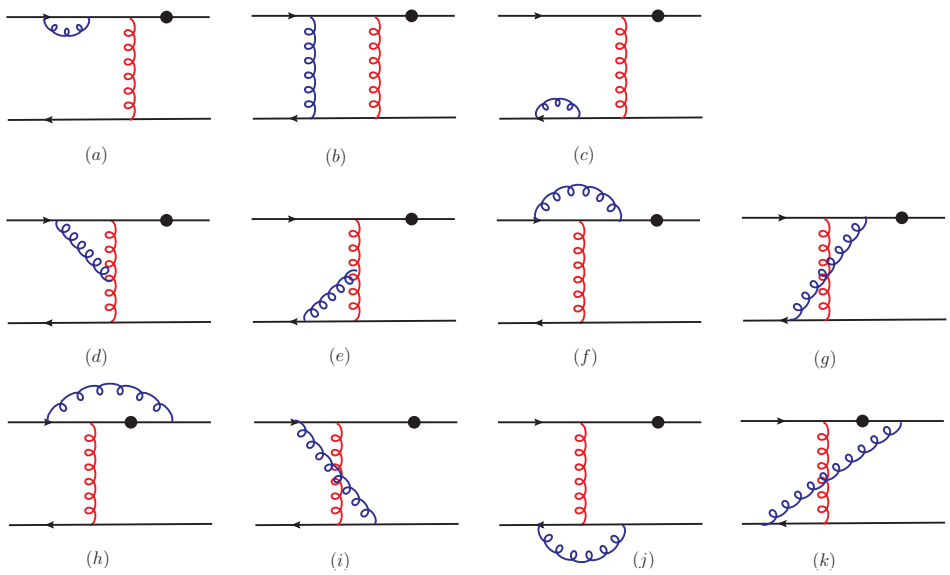

FIG. 2. $\mathcal{O}(\alpha_s)$ corrections to Fig. 1(a) with an additional gluon (blue curves) emitted from the initial ρ meson.

these three spaces in the QCD processes. We can factorize the fermion currents in the spin space by using the Fierz identity,

$$I_{ij}I_{lk}=\frac{1}{4}I_{ik}I_{lj}+\frac{1}{4}(\gamma_5)_{ik}(\gamma_5)_{lj}+\frac{1}{4}(\gamma^\alpha)_{ik}(\gamma^\alpha)_{lj} +\frac{1}{4}(\gamma_5\gamma^\alpha)_{ik}(\gamma_\alpha\gamma_5)_{lj}+\frac{1}{8}(\sigma^{\alpha\beta}\gamma_5)_{ik}(\sigma_{\alpha\beta}\gamma_5)_{lj}, \tag{6}$$

where I is the identity matrix and $\sigma^{\alpha\beta}$ is defined by $\sigma^{\alpha\beta}=i[\gamma^\alpha,\gamma^\beta]/2$, the different terms in Eq. (6) stand for different twists' contributions. The eikonal approximation is used to factorize the momenta currents in the momentum space. And at last we need to sum over all the color factors to obtain the gauge-independent high order DAs. In this section we will show the NLO factorization of the $\rho\to\pi$ transition process, according to the LO transition amplitudes expressed in Eqs. (3,4,5) for the sub-diagrams Figs. 1(a,b). We try to factorize these NLO transition amplitudes into the convolutions of the LO hard amplitudes and the NLO meson DAs.

We here firstly testify that the collinear factorization is valid at the NLO level for the Fig. 1(a), where the LO transition amplitude as given in Eq. (3) contains the T3&T2 contribution only. So we just need to consider the twist-3 DAs for the initial ρ meson and the twist-2 DA for the final state π meson in this NLO factorization proofs.

There are two types infrared divergences from $\mathcal{O}(\alpha_s)$ corrections to Fig. 1(a) induced by an additional gluon as illustrated in Fig. 2 and Fig. 4, which are distinguished by the direction of the additional gluon momentum. We firstly identify these infrared divergences for the $\mathcal{O}(\alpha_s)$ correction with the additional "blue" gluon emitted from the initial ρ meson as shown in Fig. 2, where the gluon momenta may be parallel to the rho meson momenta p_1.

It's easy to find that the amplitudes in Eqs. (7,8,9) are reducible for sub-diagrams Fig. 2(a,b,c), because we can factorize this amplitudes by simply inserting the Fierz identity. The symmetry

factor $1/2$ in the self-energy diagrams Eqs. (7,9) represent the freedom to chose the most outside vertex of the additional gluon. The soft divergences from the $l \sim (\lambda, \lambda, \lambda)$ region are canceled in these reducible amplitudes $G^{(1)}_{2a,32}(x_1; x_2), G^{(1)}_{2b,32}(x_1; x_2), G^{(1)}_{2c,32}(x_1; x_2)$, which is determined by the QCD dynamics that the soft gluon don't resolve the color structure of the rho meson.

$$\begin{aligned} G^{(1)}_{2a,32} =& \frac{1}{2}\frac{eg_s^4 C_F^2}{2}\frac{[\not{\epsilon}_{1T} M_\rho \phi_\rho^v + i M_\rho \epsilon_{\mu'\nu\rho\sigma}\gamma_5\gamma^{\mu'}\epsilon^\nu_{1T} n^\rho v^\sigma \phi_\rho^a]}{(p_1-k_2)^2(k_1-k_2)^2(p_1-k_1)^2(p_1-k_1+l)^2 l^2} \\ & \cdot\gamma^\alpha[\gamma_5 \not{p}_2 \phi_\pi^A]\gamma_\mu(\not{p}_1-\not{k}_2)\gamma_\alpha(\not{p}_1-\not{k}_1)\gamma^{\rho'}(\not{p}_1-\not{k}_1+\not{l})\gamma_{\rho'} \\ =& \frac{1}{2}\phi^{(1),v}_{\rho,a} \otimes G^{(0),v}_{a,32}(x_1; x_2) + \frac{1}{2}\phi^{(1),a}_{\rho,a} \otimes G^{(0),a}_{a,32}(x_1; x_2), \end{aligned} \tag{7}$$

$$\begin{aligned} G^{(1)}_{2b,32} =& \frac{-eg_s^4 C_F^2}{2}\frac{[\not{\epsilon}_{1T} M_\rho \phi_\rho^v + i M_\rho \epsilon_{\mu'\nu\rho\sigma}\gamma_5\gamma^{\mu'}\epsilon^\nu_{1T} n^\rho v^\sigma \phi_\rho^a]}{(p_1-k_2)^2(k_1-k_2-l)^2(p_1-k_1+l)^2(k_1-l)^2 l^2} \\ & \cdot\gamma^{\rho'}(\not{k}_1-\not{l})\gamma^\alpha[\gamma_5 \not{p}_2 \phi_\pi^A]\gamma_\mu(\not{p}_1-\not{k}_2)\gamma_\alpha(\not{p}_1-\not{k}_1+\not{l})\gamma^{\rho'} \\ =& \phi^{(1),v}_{\rho,b} \otimes G^{(0),v}_{a,32}(\xi_1, x_2) + \phi^{(1),a}_{\rho,b} \otimes G^{(0),a}_{a,32}(\xi_1, x_2), \end{aligned} \tag{8}$$

$$\begin{aligned} G^{(1)}_{2c,32} =& \frac{1}{2}\frac{eg_s^4 C_F^2}{2}\frac{[\not{\epsilon}_{1T} M_\rho \phi_\rho^v + i M_\rho \epsilon_{\mu'\nu\rho\sigma}\gamma_5\gamma^{\mu'}\epsilon^\nu_{1T} n^\rho v^\sigma \phi_\rho^a]}{(p_1-k_2)^2(k_1-k_2)^2(p_1-k_1)^2(p_1-k_1+l)^2 l^2} \\ & \cdot\gamma^{\rho'}(\not{k}_1-\not{l})\gamma_{\rho'}\not{k}_1\gamma^\alpha[\gamma_5 \not{p}_2 \phi_\pi^A]\gamma_\mu(\not{p}_1-\not{k}_2)\gamma_\alpha \\ =& \frac{1}{2}\phi^{(1),v}_{\rho,c} \otimes G^{(0),v}_{a,32}(x_1, x_2) + \frac{1}{2}\phi^{(1),a}_{\rho,c} \otimes G^{(0),a}_{a,32}(x_1, x_2), \end{aligned} \tag{9}$$

where the LO hard amplitudes $G^{(0),v}_{a,32}(\xi_1, x_2)$ and $G^{(0),a}_{a,32}(\xi_1, x_2)$ in Eq. (8) with the gluon momenta flowing into the LO hard kernel are of the following form

$$G^{(0),v}_{a,32}(\xi_1; x_2) = \frac{ieg_s^2 C_F}{2}\frac{[\not{\epsilon}_{1T} M_\rho \phi_\rho^v]\gamma^\alpha[\gamma_5 \not{p}_2 \phi_\pi^A]\gamma_\mu(\not{p}_1-\not{k}_2)\gamma_\alpha}{(p_1-k_2)^2(k_1-k_2-l)^2}, \tag{10}$$

$$G^{(0),a}_{a,32}(\xi_1; x_2) = \frac{ieg_s^2 C_F}{2}\frac{M_\rho i\epsilon_{\mu'\nu\rho\sigma}\gamma_5\gamma^{\mu'}\epsilon^\nu_{1T} n^\rho v^\sigma]\gamma^\alpha[\gamma_5 \not{p}_2 \phi_\pi^A]\gamma_\mu(\not{p}_1-\not{k}_2)\gamma_\alpha}{(p_1-k_2)^2(k_1-k_2-l)^2}. \tag{11}$$

The NLO DAs $\phi^{(1)}_\rho$ in Eqs. (7,8,9), which absorbed all the infrared singularities from those reducible sub-diagrams Figs. 2(a,b,c), can be written as the following form

$$\begin{aligned} \phi^{(1),v}_{\rho,a} =& \frac{-ig_s^2 C_F}{4}\frac{\gamma_\perp^b\gamma_{\perp b}(\not{p}_1-\not{k}_1)\gamma^{\rho'}(\not{p}_1-\not{k}_1+\not{l})\gamma_{\rho'}}{(p_1-k_1)^2(p_1-k_1+l)^2 l^2}, \\ \phi^{(1),a}_{\rho,a} =& \frac{-ig_s^2 C_F}{4}\frac{\gamma_5\gamma_\perp^{\mu'}\gamma_{\perp\mu'}\gamma_5(\not{p}_1-\not{k}_1)\gamma^{\rho'}(\not{p}_1-\not{k}_1+\not{l})\gamma_{\rho'}}{(p_1-k_1)^2(p_1-k_1+l)^2 l^2}; \\ \phi^{(1),v}_{\rho,b} =& \frac{ig_s^2 C_F}{4}\frac{\gamma_\perp^b\gamma^{\rho'}(\not{k}_1-\not{l})\gamma_{\perp b}(\not{p}_1-\not{k}_1+\not{l})\gamma_{\rho'}}{(k_1-l)^2(p_1-k_1+l)^2 l^2}, \\ \phi^{(1),a}_{\rho,b} =& \frac{ig_s^2 C_F}{4}\frac{\gamma_5\gamma_\perp^{\mu'}\gamma^{\rho'}(\not{k}_1-\not{l})\gamma_{\perp\mu'}\gamma_5(\not{p}_1-\not{k}_1+\not{l})\gamma_{\rho'}}{(k_1-l)^2(p_1-k_1+l)^2 l^2}; \\ \phi^{(1),v}_{\rho,c} =& \frac{-ig_s^2 C_F}{4}\frac{\gamma_\perp^b\gamma^{\rho'}(\not{k}_1-\not{l})\gamma_{\rho'}\not{k}_1\gamma_{\perp b}}{(k_1-l)^2(k_1)^2 l^2}, \\ \phi^{(1),a}_{\rho,c} =& \frac{-ig_s^2 C_F}{4}\frac{\gamma_5\gamma_\perp^{\mu'}\gamma^{\rho'}(\not{k}_1-\not{l})\gamma_{\rho'}\not{k}_1\gamma_{\perp\mu'}\gamma_5}{(k_1-l)^2(k_1)^2 l^2}. \end{aligned} \tag{12}$$

The additional gluons in sub-diagrams Figs. 2(d,e,f,g) generate the collinear divergences only, because one vertex of the gluon is attached to the LO hard part and then the soft region is strongly suppressed by $1/Q^2$. For these amplitudes, we choose the radiative gluon momenta being parallel to the initial rho meson momenta p_1 to evaluate the collinear divergences. All the amplitudes for those sub-diagrams in Fig. 2(d,e,f,g) are listed in Eqs. (13,15,16,17). For Fig. 2(d) we find

$$\begin{aligned} G^{(1)}_{2d,32} =& \frac{-ieg_s^4 Tr[T^aT^cT^b]f_{abc}}{2N_c}\frac{[\not\epsilon_{1T} M_\rho \phi_\rho^v + iM_\rho \epsilon_{\mu'\nu\rho\sigma}\gamma_5\gamma^{\mu'}\epsilon_{1T}^\nu n^\rho v^\sigma \phi_\rho^a]}{(p_1-k_2)^2(k_1-k_2)^2(p_1-k_1+l)^2(k_1-k_2-l)^2 l^2} \\ & \cdot\gamma^\alpha[\gamma_5 \not p_2 \phi_\pi^A]\gamma_\mu(\not p_1 - \not k_2)\gamma^\beta(\not p_1 - \not k_1 + \not l)\gamma^\gamma F_{\alpha\beta\gamma} \\ \sim& \frac{9}{16}\phi^{(1),v}_{\rho,d}\otimes[G^{(0),v}_{a,32}(x_1;x_2) - G^{(0),v}_{a,32}(\xi_1;x_2)] \\ &+\frac{9}{16}\phi^{(1),a}_{\rho,d}\otimes[G^{(0),a}_{a,32}(x_1;x_2) - G^{(0),a}_{a,32}(\xi_1;x_2)], \end{aligned} \tag{13}$$

with

$$\begin{aligned} \phi^{(1),v}_{\rho,d} &= \frac{-ig_s^2 C_F}{4}\frac{\gamma_\perp^b \gamma_{\perp b}(\not p_1 - \not k_1 + \not l)\gamma^\rho v_\rho}{(p_1-k_1+l)^2 l^2 (v\cdot l)}, \\ \phi^{(1),a}_{\rho,d} &= \frac{-ig_s^2 C_F}{4}\frac{(\gamma_5\gamma_\perp^{\mu'})(\gamma_{\perp\mu'}\gamma_5)(\not p_1 - \not k_1 + \not l)\gamma^\rho v_\rho}{(p_1-k_1+l)^2 l^2 (v\cdot l)}. \end{aligned} \tag{14}$$

In Eq. (13), we have $F_{\alpha\beta\rho'} = g_{\alpha\beta}(2k_1-2k_2-l)_{\rho'} + g_{\beta\rho'}(k_2-k_1+2l)_\alpha + g_{\rho'\alpha}(k_2-k_1-l)_\beta$, and we find that only the terms proportional to $g_{\alpha\beta}$ and $g_{\rho'\alpha}$ contribute to the LO hard kernel with $\gamma_\alpha = \gamma^-$. Then we can factorize the amplitude $G^{(1)}_{2d,32}$ into the NLO twist-3 transversal rho DAs $\phi^{(1),v}_{\rho,d}$ and $\phi^{(1),a}_{\rho,d}$ in Eq. 14, convoluted with the LO hard amplitudes $G^{(0),v}_{a,32}(x_1;x_2)$ and $G^{(0),a}_{a,32}(x_1;x_2)$, to which the gluon momenta flow or not flow in.

For Fig. 2(e) we have

$$\begin{aligned} G^{(1)}_{2e,32} =& \frac{ieg_s^4 Tr[T^aT^cT^b]f_{abc}}{2N_c}\frac{[\not\epsilon_{1T} M_\rho \phi_\rho^v + iM_\rho \epsilon_{\mu'\nu\rho\sigma}\gamma_5\gamma^{\mu'}\epsilon_{1T}^\nu n^\rho v^\sigma \phi_\rho^a]}{(p_1-k_2)^2(k_1-k_2)^2(k_1-l)^2(k_1-k_2-l)^2 l^2} \\ & \cdot\gamma^\gamma(\not k_1 - \not l)\gamma^\alpha[\gamma_5 \not p_2 \phi_\pi^A]\gamma_\mu(\not p_1 - \not k_2)\gamma^\beta F_{\alpha\beta\gamma} \\ \sim& 0, \end{aligned} \tag{15}$$

where $F_{\alpha\beta\gamma} = g_{\alpha\beta}(2k_1-2k_2-l)_\gamma + g_{\beta\gamma}(k_2-k_1-l)_\alpha + g_{\gamma\alpha}(k_2-k_1+2l)_\beta$. The possible contributions from the three terms in the tensor $F_{\alpha\beta\gamma}$ is either suppressed by the kinetics or excluded by the requirement that the Gamma matrix in the NLO amplitudes should hold the LO content $\gamma_\alpha = \gamma^-$. Then we can assume that the infrared contribution from the sub-diagram Fig. 2(e) can be neglected safely. The kinetic suppression is also happened for the amplitudes of Figs. 2(f,g), theses two sub-diagrams also do not provide infrared correction to the LO hand kernel $G^{(0),v/a}_{a,32}$, i.e.,

$$\begin{aligned} G^{(1)}_{2f,32} =& \frac{eg_s^4 Tr[T^cT^aT^cT^a]}{2N_c}\frac{[\not\epsilon_{1T} M_\rho \phi_\rho^v + iM_\rho \epsilon_{\mu'\nu\rho\sigma}\gamma_5\gamma^{\mu'}\epsilon_{1T}^\nu n^\rho v^\sigma \phi_\rho^a]}{(p_1-k_2)^2(k_1-k_2)^2(p_1-k_1+l)^2(p_1-k_2+l)^2 l^2} \\ & \cdot\gamma^\alpha[\gamma_5 \not p_2 \phi_\pi^A]\gamma_\mu(\not p_1 - \not k_2)\gamma^{\rho'}(\not p_1 - \not k_2 + \not l)\gamma_\alpha(\not p_1 - \not k_1 + \not l)\gamma_{\rho'} \\ \sim& 0, \end{aligned} \tag{16}$$

$$\begin{aligned} G^{(1)}_{2g,32} =& \frac{-eg_s^4 Tr[T^cT^aT^cT^a]}{2N_c}\frac{[\not\epsilon_{1T} M_\rho \phi_\rho^v + iM_\rho \epsilon_{\mu'\nu\rho\sigma}\gamma_5\gamma^{\mu'}\epsilon_{1T}^\nu n^\rho v^\sigma \phi_\rho^a]}{(p_1-k_2)^2(k_1-k_2-l)^2(p_1-k_2-l)^2(k_1-l)^2 l^2} \\ & \cdot\gamma_{\rho'}(\not k_1 - \not l)\gamma^\alpha[\gamma_5 \not p_2 \phi_\pi^A]\gamma_\mu(\not p_1 - \not k_2)\gamma^{\rho'}(\not p_1 - \not k_2 - \not l)\gamma_\alpha \\ \sim& 0. \end{aligned} \tag{17}$$

For sub-diagrams Figs. 2(h,i,j,k), however, the additional gluon generates the collinear divergences as well as the soft divergences, because both ends of the gluon are attached to the external quark lines. As the partner with the soft divergences, the collinear divergences are also evaluated by setting the radiative gluon momenta being parallel to the initial rho meson momenta p_1. The amplitudes for all these four sub-diagrams are given in Eqs. (18,19,20,21).

For Figs. 2(h,i) we have

$$\begin{aligned}
G^{(1)}_{2h,32} =& \frac{eg_s^4 Tr[T^c T^a T^c T^a]}{2N_c} \frac{[\not\epsilon_{1T} M_\rho \phi_\rho^v + i M_\rho \epsilon_{\mu'\nu\rho\sigma}\gamma_5\gamma^{\mu'}\epsilon_{1T}^\nu n^\rho v^\sigma \phi_\rho^a]}{(k_1-k_2)^2(p_1-k_2+l)^2(p_1-k_1+l)^2(p_2-k_2+l)^2 l^2} \\
& \cdot\gamma^\alpha[\gamma_5 \not p_2 \phi_\pi^A]\gamma^{\rho'}(\not p_2 - \not k_2 + \not l)\gamma_\mu(\not p_1 - \not k_2 + \not l)\gamma^\alpha(\not p_1 - \not k_1 + \not l)\gamma_{\rho'} \\
\sim& (-\frac{1}{8})\phi^{(1),v}_{\rho,d} \otimes G^{(0),v}_{a,32}(x_1,x_2) + (-\frac{1}{8})\phi^{(1),a}_{\rho,d} \otimes G^{(0),a}_{a,32}(x_1,x_2),
\end{aligned} \tag{18}$$

$$\begin{aligned}
G^{(1)}_{2i,32} =& \frac{-eg_s^4 Tr[T^c T^a T^c T^a]}{2N_c} \frac{[\not\epsilon_{1T} M_\rho \phi_\rho^v + i M_\rho \epsilon_{\mu'\nu\rho\sigma}\gamma_5\gamma^{\mu'}\epsilon_{1T}^\nu n^\rho v^\sigma \phi_\rho^a]}{(k_1-k_2-l)^2(p_1-k_2)^2(p_1-k_1+l)^2(k_2+l)^2 l^2} \\
& \cdot\gamma^\alpha(\not k_2 + \not l)\gamma^{\rho'}[\gamma_5 \not p_2 \phi_\pi^A]\gamma_\mu(\not p_1 - \not k_2)\gamma_\alpha(\not p_1 - \not k_1 + \not l)\gamma_{\rho'} \\
\sim& (\frac{1}{8})\phi^{(1),v}_{\rho,d} \otimes G^{(0),v}_{a,32}(\xi_1;x_2) + (\frac{1}{8})\phi^{(1),a}_{\rho,d} \otimes G^{(0),a}_{a,32}(\xi_1;x_2).
\end{aligned} \tag{19}$$

For Figs. 2(j,k), we find that $G^{(1)}_{2j,32}$ and $G^{(1)}_{2k,32}$ don't provide the NLO correction to the LO amplitude $G^{(0)}_{a,32}$, because of the confine of the Gamma matrixes to extract the LO amplitude $G^{(0)}_{a,32}$, then the infrared contribution of these two amplitudes can also be neglected safely.

$$\begin{aligned}
G^{(1)}_{2j,32} =& \frac{eg_s^4 Tr[T^c T^a T^c T^a]}{2N_c} \frac{[\not\epsilon_{1T} M_\rho \phi_\rho^v + i M_\rho \epsilon_{\mu'\nu\rho\sigma}\gamma_5\gamma^{\mu'}\epsilon_{1T}^\nu n^\rho v^\sigma \phi_\rho^a]}{(k_1-k_2)^2(p_1-k_2)^2(k_1-l)^2(k_2-l)^2 l^2} \\
& \cdot\gamma_{\rho'}(\not k_1 - \not l)\gamma_\perp^\alpha(\not k_2 - \not l)\gamma^{\rho'}[\gamma_5 \not p_2 \phi_\pi^A]\gamma_\mu(\not p_1 - \not k_2)\gamma_{\perp\alpha} \\
\sim& 0,
\end{aligned} \tag{20}$$

$$\begin{aligned}
G^{(1)}_{2k,32} =& \frac{-eg_s^4 Tr[T^c T^a T^c T^a]}{2N_c} \frac{[\not\epsilon_{1T} M_\rho \phi_\rho^v + i M_\rho \epsilon_{\mu'\nu\rho\sigma}\gamma_5\gamma^{\mu'}\epsilon_{1T}^\nu n^\rho v^\sigma \phi_\rho^a]}{(k_1-k_2-l)^2(p_1-k_2-l)^2(k_1-l)^2(p_2-k_2-l)^2 l^2} \\
& \cdot\gamma_{\rho'}(\not k_1 - \not l)\gamma_\perp^\alpha[\gamma_5 \not p_2 \phi_\pi^A]\gamma^{\rho'}(\not p_2 - \not k_2 - \not l)\gamma_\mu(\not p_1 - \not k_2 - \not l)\gamma_{\perp\alpha} \\
\sim& 0,
\end{aligned} \tag{21}$$

For the irreducible infrared amplitudes as shown in Eqs. (13,15-21), we have the following observations:

(i) We sum up the amplitudes for the irreducible sub-diagrams Figs. 2(d,f,h,i) together, in which the additional gluon is radiated from the initial up-line quark.

$$\begin{aligned}
G^{(1)}_{2up,32}(x_1;x_2) =& G^{(1)}_{2d,32}(x_1;x_2) + G^{(1)}_{2f,32}(x_1;x_2) + G^{(1)}_{2h,32}(x_1;x_2) + G^{(1)}_{2i,32}(x_1;x_2) \\
=& \phi^{(1),v}_{\rho,d} \otimes \left(\frac{7}{16}\right)\left[G^{(0),v}_{a,32}(x_1;x_2) - G^{(0),v}_{a,32}(\xi_1;x_2)\right] \\
& + \phi^{(1),a}_{\rho,d} \otimes \left(\frac{7}{16}\right)\left[G^{(0),a}_{a,32}(x_1;x_2) - G^{(0),a}_{a,32}(\xi_1;x_2)\right].
\end{aligned} \tag{22}$$

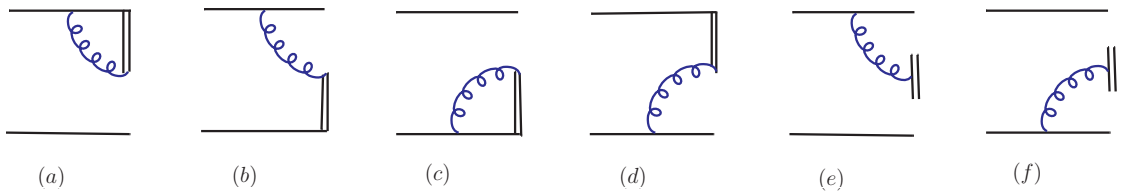

FIG. 3. $\mathcal{O}(\alpha_s)$ effective diagrams for the initial transversal rho meson wave function, which collect all the collinear divergences from the initial rho meson in the irreducible NLO quark diagrams. The vertical double line denotes the Wilson line along the light cone, whose Feynman rule is $v_\rho/(v\cdot l)$ as described in Eq. (25,26).

The summation of the amplitudes for the sub-diagrams Figs. 2(e,g,j,k), in which the additional gluon is radiated from the initial down-line quark, would give the zero infrared contribution. The infrared divergences only come from the gluon radiated from the up-line quark of rho meson as shown in Fig. 2, while the infrared contributions from the down-line quark are excluded either by the dynamics or the kinetics.

(ii) By comparing the amplitudes $G^{(1)}_{2h,32}$ with $G^{(1)}_{2i,32}$, We find that the soft divergences from the irreducible sub-diagrams Fig. 2(h) and Fig. 2(i) will be canceled completely by the simple replacement $\xi_1 \to x_1$. Combining with the cancellation of the soft divergences in the sub-diagrams Figs. 2(a,b,c), there is no soft divergence in the quark level for the Fig. 2.

(iii) The NLO corrections to the LO sub-diagram Fig. 1(a) with the collinear gluon emitted from the initial state do have the collinear divergences, but they can be absorbed into the NLO rho meson DAs $\phi^{(1),v}_{\rho,d}$ and $\phi^{(1),a}_{\rho,d}$. From Eqs. (13,16,18,19), one can write out the Feynman rules for the perturbative calculation of the NLO twist-3 transversal ρ meson wave functions $\phi^{(1),v}_{\rho,d}$ and $\phi^{(1),a}_{\rho,d}$ as a nonlocal hadronic matrix element with the structure $\gamma_\perp/2$ and $(\gamma_5\gamma_\perp)/2$ sandwiched respectively:

$$\phi^{(1),v}_{\rho,d} = \frac{1}{2N_c P_1^+}\int \frac{dy^-}{2\pi} e^{-ixp_1^+ y^-} < 0|\overline{q}(y^-)\frac{\gamma_\perp}{2}(-ig_s)\int_0^{y^-} dzv\cdot A(zv)q(0)|\rho(p_1)>, \quad (23)$$

$$\phi^{(1),a}_{\rho,d} = \frac{1}{2N_c P_1^+}\int \frac{dy^-}{2\pi} e^{-ixp_1^+ y^-} < 0|\overline{q}(y^-)\frac{\gamma_5\gamma_\perp}{2}(-ig_s)\int_0^{y^-} dzv\cdot A(zv)q(0)|\rho(p_1)> . \quad (24)$$

The integral variable z runs from 0 to ∞ for the upper eikonal line as showed in Fig. 3(a), and runs from ∞ back to y^- for the lower eikonal line as showed in Fig. 3(b). The choice of the light-cone coordinate $y^- \neq 0$ represents the fact that the collinear divergences from the sub-diagrams of Fig. 2 don't cancel exactly.

(iv) The factor $v_\rho/(v\cdot l)$ in Eq. (14) is the Feynman rule associated with the Wilson line, which is required to remain gauge invariance of the nonlocal matrix element in the NLO rho wave functions and has been included in Eqs. (23,24) of the NLO wave functions. We can retrieve this factor by Fourier transformation of the gauge field from $A(zv)$ to $A(l)$ in these NLO

wave functions:

$$\int_0^\infty dzv\cdot A(zv)\to\int dl\; e^{iz(v\cdot l+i\epsilon)}\int_0^\infty dzv\cdot\widetilde{A}(l)=i\int dl\;\frac{v_\rho}{v\cdot l}\widetilde{A}^\rho(l), \tag{25}$$

$$\int_0^{y^-} dzv\cdot A(zv)\to\int dl\; e^{iz(v\cdot l+i\epsilon)}\int_0^{y^-} dzv\cdot\widetilde{A}(l)=-i\int dl\;\frac{v_\rho}{v\cdot l}\;e^{il^+y^-}\;\widetilde{A}^\rho(l). \tag{26}$$

The Fourier factor $e^{il^+y^-}$ in Eq. (26) will lead to the function $\delta(\zeta_1-x_1+i^+/p_1^+)$, which means that the gluon momentum l has flowed into the LO hard kernel as described in Eqs. (10,11).

(v) The NLO irreducible amplitudes for Fig. 2 in the collinear region can be written as the convolutions of the NLO DAs and the LO hard amplitudes. The collinear factorization is valid for the NLO corrections for the Fig. 1(a) with the additional gluon emitted from the initial rho meson.

(vi) The sub-diagrams Figs. 3(a,b,e) are the effective-diagrams for the additional gluon radiated from the left-up quark line, the sub-diagrams Figs. 3(c,d,f) represent the effective-diagrams for the additional gluon radiated from the left-down anti-quark line. We can also sort these six effective-diagrams in Fig. 3 into three sets by the flowing of the gluon momenta: (a) the first set contains the effective diagram 3(a) and 3(c) with no gluon momenta flow into the LO hard amplitudes; (b) the second set is made of the effective diagram 3(b) and 3(d) with the gluon momenta flow into the LO hard amplitudes; and (c) the third set includes the effective diagram 3(e) and 3(f) with the gluon momenta flow partly into the LO hard amplitudes.

Now we consider the infrared divergences from $\mathcal{O}(\alpha_s)$ radiative corrections to Fig. 1(a) with the additional collinear gluon emitted from the final π meson as shown in Fig. 4, where the gluon momenta may be collinear with the pion meson momenta p_2.

Since the sub-diagrams Figs. 4(a,b,c) are reducible diagrams, we can factorize them directly by inserting the Firez identity into proper places as being done for Figs. 2(a,b,c) previously. The symmetry factor $1/2$ are also exist in $G^{(1)}_{4a,32}$ and $G^{(1)}_{4c,32}$. And the soft divergences in these reducible amplitudes $G^{(1)}_{4a,32}, G^{(1)}_{4b,32}, G^{(1)}_{4c,32}$ as given in Eqs. (27.28,29) will also be cancelled each other exactly.

$$\begin{aligned}G^{(1)}_{4a,32}=&\frac{1}{2}\frac{eg_s^4C_F^2}{2}\frac{[\not\epsilon_{1T}M_\rho\phi_\rho^v+iM_\rho\epsilon_{\mu'\nu\rho\sigma}\gamma_5\gamma^{\mu'}\epsilon_{1T}^\nu n^\rho v^\sigma\phi_\rho^a]\gamma^\alpha[\gamma_5\not p_2\phi_\pi^A]\gamma^{\rho'}}{(p_1-k_2)^2(k_1-k_2)^2(p_2-k_2)^2(p_2-k_2+l)^2l^2}\\&\cdot(\not p_2-\not k_2+\not l)\gamma_{\rho'}(\not p_2-\not k_2)\gamma_\mu(\not p_1-\not k_2)\gamma_\alpha\\=&\frac{1}{2}G^{(0)}_{a,32}(x_1;x_2)\otimes\phi^{(1),A}_{\pi,a},\end{aligned} \tag{27}$$

$$\begin{aligned}G^{(1)}_{4b,32}=&\frac{-eg_s^4C_F^2}{2}\frac{[\not\epsilon_{1T}M_\rho\phi_\rho^v+iM_\rho\epsilon_{\mu'\nu\rho\sigma}\gamma_5\gamma^{\mu'}\epsilon_{1T}^\nu n^\rho v^\sigma\phi_\rho^a]}{(p_1-k_2+l)^2(k_1-k_2+l)^2(p_2-k_2+l)^2(k_2-l)^2l^2}\\&\cdot\gamma^{\rho'}[\gamma_5\not p_2\phi_\pi^A]\gamma_{\rho'}(\not p_2-\not k_2+\not l)\gamma_\mu(\not p_1-\not k_2+\not l)\gamma_\alpha\\=&G^{(0)}_{a,32}(x_1;\xi_2)\otimes\phi^{(1),A}_{\pi,b},\end{aligned} \tag{28}$$

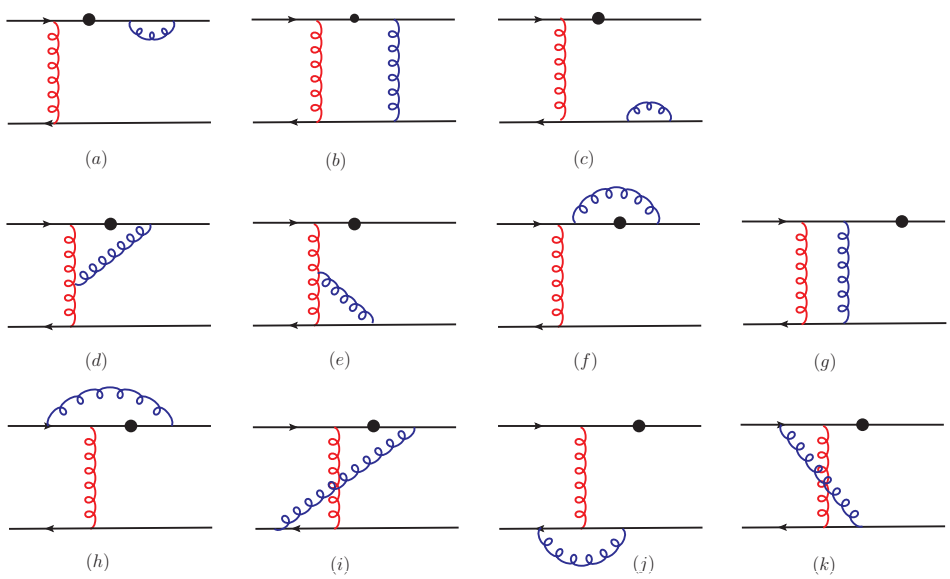

FIG. 4. $\mathcal{O}(\alpha_s)$ corrections to Fig. 1(a) with an additional gluon (blue curves) emitted from the final π meson.

$$
\begin{aligned}
G^{(1)}_{4c,32} =& \frac{1}{2}\frac{eg_s^4C_F^2}{2}\frac{[\not\epsilon_{1T}M_\rho\phi^v_\rho + iM_\rho\epsilon_{\mu'\nu\rho\sigma}\gamma_5\gamma^{\mu'}\epsilon^\nu_{1T}n^\rho v^\sigma\phi^a_\rho]\gamma^\alpha \not k_2\gamma^{\rho'}(\not k_2-\not l)}{(p_1-k_2)^2(k_1-k_2)^2(k_2-l)^2(k_2)^2l^2}\\
&\cdot\gamma_{\rho'}[\gamma_5\not p_2\phi^A_\pi]\gamma_\mu(\not p_1-\not k_2)\gamma_\alpha\\
=&\frac{1}{2}G^{(0)}_{a,32}(x_1,x_2)\otimes\phi^{(1),A}_{\pi,c},
\end{aligned}
\tag{29}
$$

where $\phi^{(1),A}_{\pi,i}$ with $i=(a,b,c)$ are the NLO DAs, which absorbed all the infrared singularities from these reducible sub-diagrams Figs. 2(a,b,c) and can be written in the following forms:

$$
\begin{aligned}
\phi^{(1),A}_{\pi,a} =& \frac{-ig_s^2C_F}{4}\frac{[\gamma_5\gamma^+]\gamma^{\rho'}(\not p_2-\not k_2+\not l)\gamma_{\rho'}(\not p_2-\not k_2)[\gamma^-\gamma_5]}{(p_2-k_2)^2(p_2-k_2+l)^2l^2};\\
\phi^{(1),A}_{\pi,b} =& \frac{ig_s^2C_F}{4}\frac{(\not k_2-\not l)\gamma^{\rho'}[\gamma_5\gamma^+]\gamma_{\rho'}(\not p_2-\not k_2+\not l)[\gamma^-\gamma_5]}{(p_2-k_2+l)^2(k_2-l)^2l^2};\\
\phi^{(1),A}_{\pi,c} =& \frac{-ig_s^2C_F}{4}\frac{[\gamma^-\gamma_5]\not k_2\gamma^{\rho'}(\not k_2-\not l)\gamma_{\rho'}[\gamma_5\gamma^+]}{(k_2-l)^2(k_2)^2l^2}.
\end{aligned}
\tag{30}
$$

The infrared singularity analysis for Fig. 2 are also valid for Fig. 4. The sub-diagrams in the second row of Fig. 4 also contain the collinear singularity only, while the third row sub-diagrams may contain both collinear and soft divergences. Before discussing the infrared behaviour of these irreducible sub-diagrams in Figs. 4(d-k), we here firstly define those LO hard amplitudes which

either appeared in Eq. 28 or will appeare in the NLO irreducible amplitudes,

$$\begin{aligned} G^{(0)}_{a,32}(x_1;\xi_2) =& \frac{ieg_s^2C_F}{2}\frac{[\not\epsilon_{1T}M_\rho\phi^v_\rho + M_\rho i\epsilon_{\mu'\nu\rho\sigma}\gamma_5\gamma^{\mu'}\epsilon^\nu_{1T}n^\rho v^\sigma]}{(p_1-k_2+l)^2(k_1-k_2+l)^2} \\ &\cdot\gamma^\alpha[\gamma_5\not p_2\phi^A_\pi]\gamma_\mu(\not p_1-\not k_2+\not l)\gamma_\alpha, \end{aligned} \tag{31}$$

$$\begin{aligned} G^{(0)}_{a,32}(x_1;\xi_2,x_2) =& \frac{ieg_s^2}{2}\frac{[\not\epsilon_{1T}M_\rho\phi^v_\rho + iM_\rho\epsilon_{\mu'\nu\rho\sigma}\gamma_5\gamma^{\mu'}\epsilon^\nu_{1T}n^\rho v^\sigma\phi^a_\rho]}{(p_1-k_2+l)^2(k_1-k_2)^2} \\ &\cdot\gamma^\alpha[\gamma_5\not p_2\phi^A_\pi]\gamma_\mu(\not p_1-\not k_2)\gamma_\alpha, \end{aligned} \tag{32}$$

$$\begin{aligned} G'^{(0)}_{a,32}(x_1;\xi_2,x_2) =& \frac{ieg_s^2}{2}\frac{[\not\epsilon_{1T}M_\rho\phi^v_\rho + iM_\rho\epsilon_{\mu'\nu\rho\sigma}\gamma_5\gamma^{\mu'}\epsilon^\nu_{1T}n^\rho v^\sigma\phi^a_\rho]}{(p_1-k_2)^2(k_1-k_2+l)^2} \\ &\cdot\gamma^\alpha[\gamma_5\not p_2\phi^A_\pi]\gamma_\mu(\not p_1-\not k_2)\gamma_\alpha. \end{aligned} \tag{33}$$

In the collinear region $l \parallel p_2$, we can find the equal relation $G^{(0)}_{a,32}(x_1;\xi_2,x_2) = G'^{(0)}_{a,32}(x_1;\xi_2,x_2)$ for the newly defined LO hard amplitudes as shown in Eqs. (32,33).

The transition amplitude for Fig. 4(d) can be written as the form of

$$\begin{aligned} G^{(1)}_{4d,32} =& \frac{-ieg_s^4Tr[T^cT^bT^a]f_{abc}}{2N_c}\frac{[\not\epsilon_{1T}M_\rho\phi^v_\rho + iM_\rho\epsilon_{\mu'\nu\rho\sigma}\gamma_5\gamma^{\mu'}\epsilon^\nu_{1T}n^\rho v^\sigma\phi^a_\rho]}{(p_1-k_2+l)^2(k_1-k_2)^2(k_1-k_2+l)^2(p_2-k_2+l)^2l^2} \\ &\cdot\gamma^\alpha[\gamma_5\not p_2\phi^A_\pi]\gamma^\beta(\not p_2-\not k_2+\not l)\gamma_\mu(\not p_1-\not k_2+\not l)\gamma^\gamma F_{\alpha\beta\gamma} \\ =& \Big[G^{(0)}_{a,32}(x_1;\xi_2,x_2) - G^{(0)}_{a,32}(x_1;\xi_2)\Big]\otimes\frac{9}{16}\phi^{(1),A}_{\pi,d}, \end{aligned} \tag{34}$$

with the tensor $F_{\alpha\beta\gamma} = g_{\alpha\beta}(k_1-k_2-l)_\gamma + g_{\beta\gamma}(k_1-k_2+2l)_\alpha + g_{\gamma\alpha}(2k_2-2k_1-l)_\beta$, in which only terms proportional to $g_{\beta\gamma}$ and $g_{\gamma\alpha}$ contribute to the LO hard kernel $G^{(0)}_{a,32}$. The NLO twist-2 pion DA $\phi^{(1),A}_{\pi,d}$ is defined in the following form

$$\phi^{(1),A}_{\pi,d} = \frac{-ig_s^2C_F}{4}\frac{[\gamma_5\gamma^+]\gamma^\rho(\not p_2-\not k_2+\not l)[\gamma^-\gamma_5]n_{\rho'}}{(p_2-k_2+l)^2l^2(n\cdot l)}. \tag{35}$$

Here the eikonal approximation has been employed to obtain the convolution forms for these irreducible amplitudes.

For Fig. 4(e), similarly, we have

$$\begin{aligned} G^{(1)}_{4e,32} =& \frac{ieg_s^4Tr[T^cT^bT^a]f_{abc}}{2N_c}\frac{[\not\epsilon_{1T}M_\rho\phi^v_\rho + iM_\rho\epsilon_{\mu'\nu\rho\sigma}\gamma_5\gamma^{\mu'}\epsilon^\nu_{1T}n^\rho v^\sigma\phi^a_\rho]}{(p_1-k_2)^2(k_1-k_2)^2(k_1-k_2+l)^2(k_2-l)^2l^2} \\ &\cdot\gamma^\alpha(\not k_2-\not l)\gamma^\beta[\gamma_5\not p_2\phi^A_\pi]\gamma_\mu(\not p_1-\not k_2)\gamma^\gamma F_{\alpha\beta\gamma} \\ =& \Big[G^{(0)}_{a,32}(x_1;x_2) - G'^{(0)}_{a,32}(x_1;\xi_2,x_2)\Big]\otimes\frac{9}{16}\phi^{(1),A}_{\pi,e}, \end{aligned} \tag{36}$$

where $F_{\alpha\beta\gamma} = g_{\alpha\beta}(k_1-k_2+2l)_\gamma + g_{\beta\gamma}(k_1-k_2-l)_\alpha + g_{\gamma\alpha}(2k_2-2k_1-l)_\beta$, and only the terms proportional to $g_{\beta\gamma}$ and $g_{\gamma\alpha}$ contribute to the LO hard kernel $G^{(0)}_{a,32}$. The NLO twist-2 pion DA $\phi^{(1),A}_{\pi,e}$ is defined in the form of

$$\phi^{(1),A}_{\pi,e} = \frac{ig_s^2C_F}{4}\frac{[\gamma_5\gamma^+]\gamma^\rho(\not k_2-\not l)[\gamma^-\gamma_5]n_{\rho'}}{(k_2-l)^2l^2(n\cdot l)}, \tag{37}$$

where the additional gluon is emitted from the right-down anti-parton line. Then the amplitudes for the remaining irreducible sub-diagrams in Fig. 4 can be written with the definitions in Eqs. (31,32,33,35,37):

$$\begin{aligned} G^{(1)}_{4f,32} =& \frac{eg_s^4 C_F^2 N_c}{2N_c} \frac{[\not\epsilon_{1T} M_\rho \phi_\rho^v + i M_\rho \epsilon_{\mu'\nu\rho\sigma}\gamma_5\gamma^{\mu'}\epsilon_{1T}^\nu n^\rho v^\sigma \phi_\rho^a]}{(p_1-k_2)^2(k_1-k_2)^2(p_2-k_2+l)^2 l^2 (p_1-k_2+l)^2} \\ & \cdot\gamma^\alpha[\gamma_5 \not p_2 \phi_\pi^A]\gamma^{\rho'}(\not p_2 - \not k_2 + \not l)\gamma_\mu(\not p_1 - \not k_2 + \not l)\gamma_{\rho'}(\not p_1 - \not k_2)\gamma_\alpha \\ =& \Big[G^{(0)}_{a,32}(x_1;x_2) - G^{(0)}_{a,32}(x_1;\xi_2,x_2)\Big] \otimes \phi^{(1),A}_{\pi,d}, \end{aligned} \tag{38}$$

$$\begin{aligned} G^{(1)}_{4g,32} =& \frac{-eg_s^4 C_F^2 N_c}{2N_c} \frac{[\not\epsilon_{1T} M_\rho \phi_\rho^v + i M_\rho \epsilon_{\mu'\nu\rho\sigma}\gamma_5\gamma^{\mu'}\epsilon_{1T}^\nu n^\rho v^\sigma \phi_\rho^a]}{(p_1-k_2)^2(k_1-k_2+l)^2(k_2-l)^2 l^2 (p_1-k_2+l)^2} \\ & \cdot\gamma^\alpha(\not k_2 - \not l)\gamma^{\rho'}[\gamma_5 \not p_2 \phi_\pi^A]\gamma_\mu(\not p_1 - \not k_2)\gamma_{\rho'}(\not p_1 - \not k_2 + \not l)\gamma_\alpha \\ =& \Big[G'^{(0)}_{a,32}(x_1;\xi_2,x_2) - G^{(0)}_{a,32}(x_1;\xi_2)\Big] \otimes \phi^{(1),A}_{\pi,e}, \end{aligned} \tag{39}$$

$$\begin{aligned} G^{(1)}_{4h,32} =& \frac{eg_s^4 Tr[T^c T^a T^c T^a]}{2N_c} \frac{[\not\epsilon_{1T} M_\rho \phi_\rho^v + i M_\rho \epsilon_{\mu'\nu\rho\sigma}\gamma_5\gamma^{\mu'}\epsilon_{1T}^\nu n^\rho v^\sigma \phi_\rho^a]}{(p_1-k_2+l)^2(k_1-k_2)^2(p_2-k_2+l)^2 l^2 (p_1-k_1+l)^2} \\ & \cdot\gamma^\alpha[\gamma_5 \not p_2 \phi_\pi^A]\gamma^{\rho'}(\not p_2 - \not k_2 + \not l)\gamma_\mu(\not p_1 - \not k_2 + \not l)\gamma_\alpha(\not p_1 - \not k_1 + \not l)\gamma_{\rho'} \\ =& G^{(0)}_{a,32}(x_1;\xi_2,x_2) \otimes (-\frac{1}{8})\phi^{(1),A}_{\pi,d}, \end{aligned} \tag{40}$$

$$\begin{aligned} G^{(1)}_{4i,32} =& \frac{-eg_s^4 Tr[T^c T^a T^c T^a]}{2N_c} \frac{[\not\epsilon_{1T} M_\rho \phi_\rho^v + i M_\rho \epsilon_{\mu'\nu\rho\sigma}\gamma_5\gamma^{\mu'}\epsilon_{1T}^\nu n^\rho v^\sigma \phi_\rho^a]}{(p_1-k_2+l)^2(k_1-k_2+l)^2(p_2-k_2+l)^2 l^2 (k_1+l)^2} \\ & \cdot\gamma_{\rho'}(\not k_1 + \not l)\gamma^\alpha[\gamma_5 \not p_2 \phi_\pi^A]\gamma^{\rho'}(\not p_2 - \not k_2 + \not l)\gamma_\mu(\not p_1 - \not k_2 + \not l)\gamma_\alpha \\ =& 0, \end{aligned} \tag{41}$$

$$\begin{aligned} G^{(1)}_{4j,32} =& \frac{eg_s^4 Tr[T^c T^a T^c T^a]}{2N_c} \frac{[\not\epsilon_{1T} M_\rho \phi_\rho^v + i M_\rho \epsilon_{\mu'\nu\rho\sigma}\gamma_5\gamma^{\mu'}\epsilon_{1T}^\nu n^\rho v^\sigma \phi_\rho^a]\gamma_{\rho'}(\not k_1 - \not l)\gamma^\alpha}{(p_1-k_2)^2(k_1-k_2)^2(k_2-l)^2 l^2 (k_1-l)^2} \\ & \cdot(\not k_2 - \not l)\gamma^{\rho'}[\gamma_5 \not p_2 \phi_\pi^A]\gamma_\mu(\not p_1 - \not k_2)\gamma_\alpha \\ =& 0, \end{aligned} \tag{42}$$

$$\begin{aligned} G^{(1)}_{4k,32} =& \frac{-eg_s^4 Tr[T^c T^a T^c T^a]}{2N_c} \frac{[\not\epsilon_{1T} M_\rho \phi_\rho^v + i M_\rho \epsilon_{\mu'\nu\rho\sigma}\gamma_5\gamma^{\mu'}\epsilon_{1T}^\nu n^\rho v^\sigma \phi_\rho^a]}{(p_1-k_2)^2(k_1-k_2+l)^2(k_2-l)^2 l^2 (p_1-k_1-l)^2} \\ & \cdot\gamma^\alpha(\not k_2 - \not l)\gamma^{\rho'}[\gamma_5 \not p_2 \phi_\pi^A]\gamma_\mu(\not p_1 - \not k_2)\gamma_\alpha(\not p_1 - \not k_1 - \not l)\gamma_{\rho'} \\ =& G'^{(0)}_{a,32}(x_1;\xi_2,x_2) \otimes (\frac{1}{8})\phi^{(1),A}_{\pi,e}. \end{aligned} \tag{43}$$

The infrared contributions from the NLO amplitudes $G^{(1)}_{4j,32}$ and $G^{(1)}_{4j,32}$ are zero, since the Gamma matrixes in these two amplitudes are $\gamma^\alpha = \gamma^\alpha_\perp$ instead of the $\gamma^\alpha = \gamma^-$ for the LO amplitudes.

In order to investigate the NLO collinear factorization of the Fig. 4 and to extracte the NLO twist-2 pion meson DA, we make the summation over all the irreducible amplitudes in Fig. 4 into two sets: the first set includes the sub-diagrams with the gluon radiated from the right-up quark line

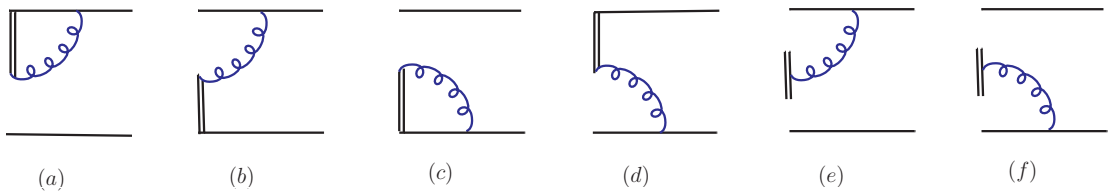

FIG. 5. $\mathcal{O}(\alpha_s)$ effective diagrams for the final pion meson wave function, with vertical double line denoting the Wilson line along the light cone, whose Feynman rule is $n_{\rho'}/(n\cdot l)$.

of the final pion meson, while the second set containes the sub-diagrams with the gluon radiated from the right-down quark line.

We firstly sum up the infrared amplitudes for the irreducible sub-diagrams in Figs. 4(d,f,h,i) with the gluon radiated from the right-up quark line:

$$\begin{aligned} G^{(1)}_{4\text{up},32}(x_1;x_2) &= G^{(1)}_{4d,32}(x_1;x_2)+G^{(1)}_{4f,32}(x_1;x_2)+G^{(1)}_{4h,32}(x_1;x_2)+G^{(1)}_{4i,32}(x_1;x_2) \\ &= \left[G^{(0)}_{a,32}(x_1;x_2)-\frac{9}{16}G^{(0)}_{a,32}(x_1;\xi_2)-\frac{9}{16}G^{(0)}_{a,32}(x_1;x_2,\xi_2)\right]\otimes\phi^{(1),A}_{\pi,d}; \end{aligned} \tag{44}$$

For the second set of the irreducible sub-diagrams in Figs. 4(e,g,j,k)(where the gluon radiated from the right-down anti-quark line), similarly, we make the summation and then find the infrared amplitude:

$$\begin{aligned} G^{(1)}_{4\text{down},32}(x_1;x_2) &= G^{(1)}_{4e,32}(x_1;x_2)+G^{(1)}_{4h,32}(x_1;x_2)+G^{(1)}_{4j,32}(x_1;x_2)+G^{(1)}_{4k,32}(x_1;x_2) \\ &= \left[-G^{(0)}_{a,32}(x_1;\xi_2)+\frac{9}{16}G^{(0)}_{a,32}(x_1;x_2)+\frac{9}{16}G^{(0)}_{a,32}(x_1;x_2,\xi_2)\right]\otimes\phi^{(1),A}_{\pi,e}. \end{aligned} \tag{45}$$

Because the IR singularities in Eqs. (41,42) are suppressed, then the soft divergences in Eq. (40) and Eq. (43) from the collinear region can't be cancelled by their counterparts described in Eq. (41) and Eq. (42) respectively. But these remained soft divergences in Eqs. (40,43) could be canceled each other exactly, because the NLO DA $\phi^{(1),A}_{\pi,d}$ in Eq. (35) is equivalent to the DA $\phi^{(1),A}_{\pi,e}$ in Eq. (37). At the quark level, finally, no soft divergences are left after summation of the NLO contributions from all the sub-diagrams as shown in Fig. 4.

All the remaining collinear divergences can be absorbed into the NLO twist-2 pion meson DA $\phi^{(1),A}_{\pi}$. From the expressions as given in Eqs. (34,36,38,39,40,43), we can define the Feynman rules for the perturbative calculation of the twist-2 pion wave function $\phi^{(1),A}_{\pi}$ as a nonlocal hadronic matrix element with the structure $(\gamma^-\gamma_5)/2$ sandwiched:

$$\phi^{(1),A}_{\pi}=\frac{1}{2N_cP_2^-}\int\frac{dy^+}{2\pi}e^{-ixp_2^-y^+}<\pi(p_2)|\overline{q}(y^+)(-ig_s)\int_0^{y^+}dzn\cdot A(zn)\frac{\gamma^-\gamma_5}{2}q(0)|0>, \tag{46}$$

which has the same form as the in the $\pi\gamma^\star\to\pi$[9]. The relevant effective diagrams for the pion meson wave function are also showed in Fig. 5, and here only the first four diagrams in Fig. 5 are useful to this sort NLO corrections described in Fig. 4 because the corrections with the gluon momentum partly flowing into LO hard kernel are cancelled in Eqs. (44,45). We can also derived the Feynman rule ($n_{\rho'}/(n\cdot l)$) for the Wilson line in Fig. 5 from the $\mathcal{O}(\alpha_s)$ component of the pion wave function by the similar Fourier transformation as for Fig. 3. Then collinear factorization is therefore valid for the NLO corrections for the Fig. 1(a) when the additional gluon emitted from the final pion meson.

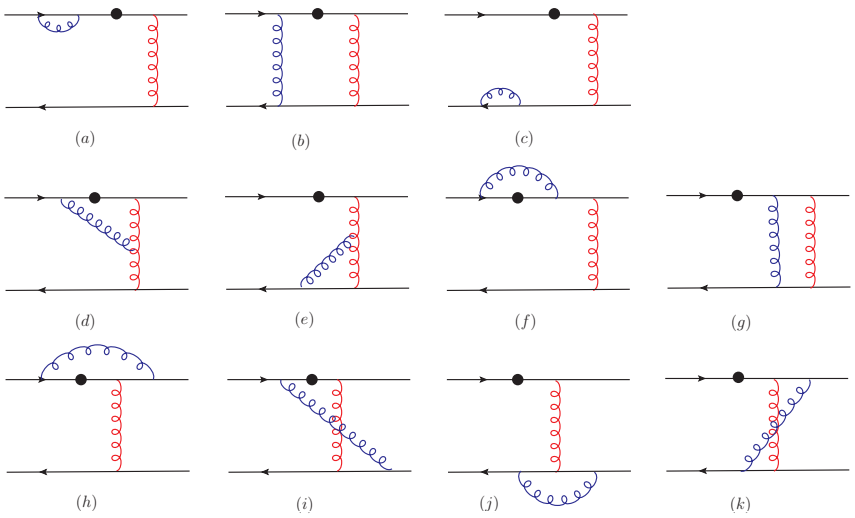

FIG. 6. $\mathcal{O}(\alpha_s)$ correction to Fig. 1(b) with the additional gluon (blue curves) emitted from the initial ρ meson.

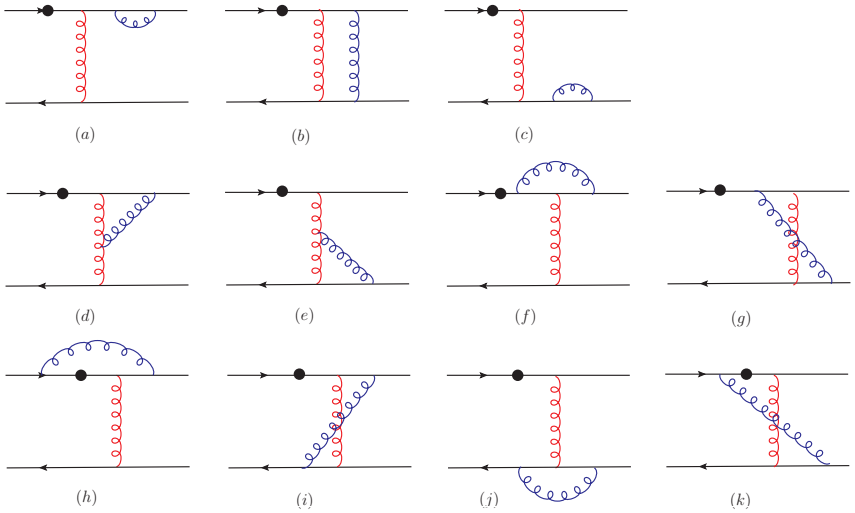

FIG. 7. $\mathcal{O}(\alpha_s)$ corrections to Fig. 1(b) with the additional gluon (blue curves) emitted from the final π meson.

C. $\mathcal{O}(\alpha_s)$ correction to Fig. 1(b)

In this subsection, we study the feasibility of the collinear factorization for the NLO corrections to Fig. 1(b) with the same approach as we did for Fig. 1(a). With the requirement to hold the LO contents as shown in Eqs. (4,5) in the NLO factorization proof, we will consider both the T2&T3 and T3&T2 sets for the DAs of the initial and final state meson in the NLO transition process as illustrated in Fig. 6 and Fig. 7. We try to use the collinear factorization approach to separate the infrared divergences of the amplitudes for Fig. 6 and Fig. 7 with the additional blue gluons radiated from the initial rho meson and final pion meson respectively.

Firstly, the reducible sub-diagrams Figs. 6(a,b,c) and Figs. 7(a,b,c) are factorized easily by

simple inserting of the Fierz identity defied in Eq. 6. And the soft divergences will be canceled exactly in these reducible amplitudes similarly as we verified for Figs. 2(a,b,c)and Figs. 4(a,b,c). We can then extract out the NLO twist-2 transversal rho meson DA's and the NLO twist-3 pion meson DA's in the following forms:

$$\begin{aligned}
\phi^{(1),T}_{\rho,a} &= \frac{-ig_s^2 C_F}{8}\frac{[\gamma^a_\perp\gamma^-][\gamma_{\perp a}\gamma^+](\not p_1-\not k_1)\gamma^{\rho'}(\not p_1-\not k_1+\not l)\gamma_{\rho'}}{(p_1-k_1)^2(p_1-k_1+l)^2l^2},\\
\phi^{(1),T}_{\rho,b} &= \frac{ig_s^2 C_F}{8}\frac{[\gamma^a_\perp\gamma^-]\gamma_{\rho'}(\not k_1-\not l)[\gamma_{\perp a}\gamma^+](\not p_1-\not k_1+\not l)\gamma^{\rho'}}{(k_1-l)^2(p_1-k_1+l)^2l^2},\\
\phi^{(1),T}_{\rho,c} &= \frac{-ig_s^2 C_F}{8}\frac{[\gamma^a_\perp\gamma^-]\gamma^{\rho'}(\not k_1-\not l)\gamma_{\rho'}\not k_1[\gamma_{\perp a}\gamma^+]}{(k_1)^2(k_1-l)^2l^2};
\end{aligned} \tag{47}$$

$$\begin{aligned}
\phi^{(1),P}_{\pi,a} &= \frac{-ig_s^2 C_F}{4}\frac{\gamma_5\gamma^{\rho'}(\not p_2-\not k_2+\not l)\gamma_{\rho'}(\not p_2-\not k_2)\gamma_5}{(p_2-k_2)^2(p_2-k_2+l)^2l^2},\\
\phi^{(1),P}_{\pi,b} &= \frac{ig_s^2 C_F}{4}\frac{(\not k_2-\not l)\gamma_{\rho'}\gamma_5\gamma^{\rho'}(\not p_2-\not k_2+\not l)\gamma_5}{(k_2-l)^2(p_2-k_2+l)^2l^2},\\
\phi^{(1),P}_{\pi,c} &= \frac{-ig_s^2 C_F}{4}\frac{\gamma_5\not k_2\gamma^{\rho'}(\not k_2-\not l)\gamma_{\rho'}\gamma_5}{(k_1)^2(k_1-l)^2l^2}.
\end{aligned} \tag{48}$$

Secondly, the NLO transversal NLO twist-2 rho meson DA $\phi^{(1),T}_{\rho,d}$ and the NLO twist-3 pion meson DAs $\phi^{(1),P}_{\pi,d}$) can be extracted from the irreducible sub-diagrams Figs. 6(d,e,f,g) and Figs. 7(d,e,f,g) respectively and are of the following form:

$$\phi^{(1),T}_{\rho,d} = \frac{-ig_s^2 C_F}{8}\frac{[\gamma^a_\perp\gamma^-][\gamma_{\perp a}\gamma^+](\not p_1-\not k_1+\not l)\gamma^\rho v_\rho}{(p_1-k_1+l)^2l^2(v\cdot l)}. \tag{49}$$

$$\phi^{(1),P}_{\pi,d} = \frac{-ig_s^2 C_F}{4}\frac{\gamma_5\gamma^\rho(\not p_2-\not k_2+\not l)\gamma_5 v_\rho}{(p_2-k_2+l)^2l^2(v\cdot l)}, \tag{50}$$

Thirdly, the NLO transversal NLO rho meson DA $\phi^{(1),T/v/a}_{\rho,e}$ and the NLO twist-3 pion meson DAs $\phi^{(1),P}_{\pi,e}$ can also be extracted from the irreducible sub-diagrams Figs. 6(h,i,j,k) and Figs. 7(h,i,j,k) respectively, and can be written in the following form:

$$\begin{aligned}
\phi^{(1),T}_{\rho,e} &= \frac{ig_s^2 C_F}{8}\frac{[\gamma^a_\perp\gamma^-]\gamma^\rho(\not k_1-\not l)[\gamma_{\perp a}\gamma^+]v_\rho}{(k_1-l)^2l^2(v\cdot l)}\left[1-\frac{(k_1-k_2)^2}{(k_1-k_2-l)^2}\right],\\
\phi^{(1),v}_{\rho,e} &= \frac{ig_s^2 C_F}{4}\frac{\gamma^b_\perp\gamma^\rho(\not k_1-\not l)\gamma_a v_\rho}{(k_1-l)^2l^2(v\cdot l)}\left[1-\frac{(k_1-k_2)^2}{(k_1-k_2-l)^2}\right],\\
\phi^{(1),a}_{\rho,e} &= \frac{ig_s^2 C_F}{4}\frac{[\gamma_5\gamma^{\mu'}_\perp]\gamma^\rho(\not k_1-\not l)[\gamma_{\perp\mu'}\gamma_5]v_\rho}{(k_1-l)^2l^2(v\cdot l)}\left[1-\frac{(k_1-k_2)^2}{(k_1-k_2-l)^2}\right];
\end{aligned} \tag{51}$$

$$\phi^{(1),P}_{\pi,e} = \frac{ig_s^2 C_F}{4}\frac{\gamma_5(\not k_2-\not l)\gamma^\rho\gamma_5 n_\rho}{(k_2-l)^2l^2(n\cdot l)}. \tag{52}$$

The hard LO amplitude $G^{(0)}_{b,23}(\xi_1,x_2)$, $G^{(0),v/a}_{b,32}(\xi_1,x_2)$ and $G^{(\prime)(0)}_{b,23}(x_1,\xi_1,x_2)$ with the gluon momenta flowing or partly flowing into the original LO hard amplitudes, are defined in the collinear

region $l \parallel p_1$ for Fig. 6 in the following form:

$$G^{(0)}_{b,23}(\xi_1;x_2) = \frac{ieg_s^2C_F}{2}\frac{[\not\epsilon_{1T}\not p_1\phi_\rho^T]\gamma^\alpha[\gamma_5 m_\pi^0\phi_\pi^P]\gamma_\alpha(\not p_2-\not k_1+\not l)\gamma_\mu}{(p_2-k_1+l)^2(k_1-k_2-l)^2}, \tag{53}$$

$$G^{(0),v}_{b,32}(\xi_1;x_2) = \frac{ieg_s^2C_F}{2}\frac{[\not\epsilon_{1T}M_\rho\phi_\rho^v]\gamma^\alpha[\gamma_5\not p_2\phi_\pi^A]\gamma_\alpha(\not p_2-\not k_1+\not l)\gamma_\mu}{(p_2-k_1+l)^2(k_1-k_2-l)^2}, \tag{54}$$

$$G^{(0),a}_{b,32}(\xi_1;x_2) = \frac{ieg_s^2C_F}{2}\frac{[M_\rho i\epsilon_{\mu'\nu\rho\sigma}\gamma_5\gamma^{\mu'}\epsilon_{1T}^\nu n^\rho v^\sigma]\gamma^\alpha[\gamma_5\not p_2\phi_\pi^A]\gamma_\alpha(\not p_2-\not k_1+\not l)\gamma_\mu}{(p_2-k_1+l)^2(k_1-k_2-l)^2}, \tag{55}$$

$$G^{(0)}_{b,23}(x_1,\xi_1;x_2) = \frac{ieg_s^2C_F}{2}\frac{[\not\epsilon_{1T}\not p_1\phi_\rho^T]\gamma^\alpha[\gamma_5 m_\pi^0\phi_\pi^P]\gamma_\alpha(\not p_2-\not k_1+\not l)\gamma_\mu}{(p_2-k_1+l)^2(k_1-k_2)^2}, \tag{56}$$

$$G'^{(0)}_{b,23}(x_1,\xi_1;x_2) = \frac{ieg_s^2C_F}{2}\frac{[\not\epsilon_{1T}\not p_1\phi_\rho^T]\gamma^\alpha[\gamma_5 m_\pi^0\phi_\pi^P]\gamma_\alpha(\not p_2-\not k_1)\gamma_\mu}{(p_2-k_1)^2(k_1-k_2-l)^2}, \tag{57}$$

where the γ^α in Eqs. (56,57) could be γ^+ or $\gamma^\alpha_\perp$. When we set $\gamma^\alpha = \gamma^+$, the amplitude $G^{(0)}_{b,23}(x_1,\xi_1,x_2)$ becomes $G^{(0),L}_{b,23}(x_1,\xi_1,x_2)$, while $G'^{(0)}_{b,23}(x_1,\xi_1,x_2)$ becomes $G'^{(0),L}_{b,23}(x_1,\xi_1,x_2)$. When we choose $\gamma^\alpha = \gamma^\alpha_\perp$, the amplitude $G^{(0)}_{b,23}(x_1,\xi_1,x_2)$ becomes $G^{(0),T}_{b,23}(x_1,\xi_1,x_2)$, while $G'^{(0)}_{b,23}(x_1,\xi_1,x_2)$ becomes $G'^{(0),T}_{b,23}(x_1,\xi_1,x_2)$. And we can find that in the collinear region $l \parallel p_1$, these two newly defined LO amplitudes in Eqs. (56,56) should be equal.

From the irreducible sub-diagrams of Fig. 7 in the collinear region $l \parallel p_2$, the LO hard amplitudes $G^{(0)}_{b,23/32}(x_1;\xi_2)$ and $G^{(\prime\prime)(0)}_{b,32}(x_1;\xi_2,x_2)$ with the gluon momentum flowing or partly flowing into the original LO hard amplitudes can be defined in the following form:

$$G^{(0)}_{b,23}(x_1;\xi_2) = \frac{ieg_s^2C_F}{2}\frac{[\not\epsilon_{1T}\not p_1\phi_\rho^T]\gamma^\alpha[\gamma_5 m_\pi^0\phi_\pi^P]\gamma_\alpha(\not p_2-\not k_1)\gamma_\mu}{(p_2-k_1)^2(k_1-k_2-l)^2}, \tag{58}$$

$$\begin{aligned} G^{(0)}_{b,32}(x_1;\xi_2) = {}& \frac{ieg_s^2C_F}{2}\frac{[\not\epsilon_{1T}M_\rho\phi_\rho^v + iM_\rho\epsilon_{\mu'\nu\rho\sigma}\gamma_5\gamma^{\mu'}\epsilon_{1T}^\nu n^\rho v^\sigma\phi_\rho^a]}{(p_2-k_1)^2(k_1-k_2-l)^2} \\ & \cdot\gamma^\alpha[\gamma_5\not p_2\phi_\pi^A]\gamma_\alpha(\not p_2-\not k_1)\gamma_\mu, \end{aligned} \tag{59}$$

$$\begin{aligned} G^{(0)}_{b,32}(x_1;\xi_2,x_2) = {}& \frac{ieg_s^2C_F}{2}\frac{[\not\epsilon_{1T}M_\rho\phi_\rho^v + iM_\rho\epsilon_{\mu'\nu\rho\sigma}\gamma_5\gamma^{\mu'}\epsilon_{1T}^\nu n^\rho v^\sigma\phi_\rho^a]}{(p_2-k_1+l)^2(k_1-k_2)^2} \\ & \cdot\gamma^\alpha[\gamma_5\not p_2\phi_\pi^A]\gamma_\alpha(\not p_2-\not k_1)\gamma_\mu, \end{aligned} \tag{60}$$

$$\begin{aligned} G''^{(0)}_{b,32}(x_1;\xi_2,x_2) = {}& \frac{ieg_s^2C_F}{2}\frac{[\not\epsilon_{1T}M_\rho\phi_\rho^v + iM_\rho\epsilon_{\mu'\nu\rho\sigma}\gamma_5\gamma^{\mu'}\epsilon_{1T}^\nu n^\rho v^\sigma\phi_\rho^a]}{(p_2-k_1+l)^2(k_1-k_2+l)^2} \\ & \cdot\gamma^\alpha[\gamma_5\not p_2\phi_\pi^A]\gamma_\alpha(\not p_2-\not k_1)\gamma_\mu. \end{aligned} \tag{61}$$

By summing up the amplitudes from those irreducible sub-diagrams Figs. 6(d,e,f,g,h,i,j,k), the total NLO amplitudes with the crossed-twist DAs T2&T3 (i.e. the NLO set-I amplitude) can be written in a convolution of the NLO rho wave function and the LO hard amplitudes, with the gluon

momentum not flowing, flowing or partly flowing into the LO hard kernels:

$$G^{(1)}_{6,23}(x_1;x_2) = \phi^{(1),T}_{\rho,d} \otimes \Big\{ G^{(0),L}_{b,23}(x_1;x_2) - \frac{9}{16} G^{(0),L}_{b,23}(\xi_1;x_2) - \frac{9}{16} G^{(0),L}_{b,23}(x_1,\xi_1;x_2) + G^{(0),T}_{b,23}(x_1;x_2) - G^{(0),T}_{b,23}(\xi_1;x_2) + \frac{1}{8} G^{(0),T}_{b,23}(x_1,\xi_1;x_2) \Big\} + \phi^{(1),T}_{\rho,e} \otimes \Big\{ -G^{(0),L}_{b,23}(\xi_1;x_2) + \frac{9}{16} G^{(0),L}_{b,23}(x_1;x_2) + \frac{9}{16} G^{(0),L}_{b,23}(x_1,\xi_1;x_2) + G^{(0),T}_{b,23}(x_1;x_2) - G^{(0),T}_{b,23}(\xi_1;x_2) - \frac{1}{8} G^{(0),T}_{b,23}(x_1,\xi_1;x_2) \Big\}. \quad (62)$$

It's easy to find that the soft divergences from the collinear region for these irreducible amplitudes are canceled each other. At the quark level, consequently, there is no soft divergence left after the summation for the contributions from all sub-diagrams in Fig. 6 with the case of the T2&T3 DAs. The collinear divergences, generated from the gluon radiated from the up-line quark and the down-line anti-quark of the initial rho meson in Fig. 6, can be absorbed into the NLO twist-2 rho meson DA $\phi^{(1),T}_{\rho,d/e}$, which is written in the following nonlocal hadronic matrix element in $\mathbf{b}$ space with the structure $(\gamma^b_\perp \gamma^+)/4$ sandwiched:

$$\phi^{(1),T}_{\rho} = \frac{1}{2N_c P_1^+} \int \frac{dy^-}{2\pi} e^{-ixp_1^+ y^-} < 0|\overline{q}(y^-) \frac{\gamma^b_\perp \gamma^+}{4} (-ig_s) \int_0^{y^-} dz v \cdot A(zv) q(0)|\rho(p_1) > . \quad (63)$$

We then give a short summary for the NLO Set-II amplitudes with the crossed-twist DAs T3&T2 for the sub-diagrams Figs. 6(d,e,f,g,h,i,j,k). After the summation, the total infrared divergences from the NLO corrections to the LO hard amplitude $G^{(0)}_{b,32}(x_1;x_2)$ in the $l \parallel p_1$ region can be written in the following form:

$$G^{(1)}_{6,32}(x_1;x_2) = \phi^{(1),v}_{\rho,e} \otimes \Big\{ 2G^{(0),v}_{b,23}(x_1;x_2) + 2G^{(0),v}_{b,23}(\xi_1;x_2) \Big\}. \quad (64)$$

We find that the infrared divergences from the Set-II amplitudes for sub-diagrams Figs. 6(d,g,h,i), with the additional gluon radiated from the right-up quark line, are suppressed by the kinetic constraints, then only the sub-diagrams Figs. 6(e,g,j,k) generate infrared divergent corrections to the Set-II LO amplitudes $G^{(0)}_{b,32}(x_1;x_2)$ with T3&T2 DAs. The soft divergences from the sub-diagrams with the gluon radiated from the left-down anti-quark line were canceled exactly. Only the collinear divergences, generated from the gluon radiated from the left-down anti-quark of the initial rho meson in Fig. 6, will be absorbed into the NLO twist-3 rho meson DA $\phi^{(1),v}_{\rho}$. Then we can factorize the Set-II irreducible amplitudes for Fig. 6 in the collinear region as the convolutions of the NLO twist-3 DA and LO hard amplitudes. The collinear factorization is therefore valid for the NLO Set-II corrections for the Fig. 1(b) with the additional gluon emitted from the initial rho meson.

Now, we elaborate the factorization for the infrared divergences in the irreducible sub-diagrams Fig. 7(d,e,f,g,h,i,j,k), in which the additional blue gluons are radiated from the final pion meson. The total NLO corrections for the Set-I amplitudes of the sub-diagrams Figs. 7(d,e,f,g,h,i,j,k) with the T2&T3 DAs from the $l \parallel p_2$ region are also summed over and can be written in the following convolution form:

$$G^{(1)}_{7,23}(x_1;x_2) = \phi^{(1),P}_{\pi,d} \otimes \Big\{ \frac{7}{16} \Big[G^{(0),L}_{b,23}(x_1;x_2) - G^{(0),L}_{b,23}(x_1;\xi_2) \Big] - \frac{9}{16} \Big[G^{(0),T}_{b,23}(x_1;x_2) - G^{(0),T}_{b,23}(x_1;\xi_2) \Big] \Big\} + \phi^{(1),P}_{\pi,e} \otimes \frac{25}{16} \Big[G^{(0),T}_{b,23}(x_1;x_2) - G^{(0),T}_{b,23}(x_1;\xi_2) \Big]. \quad (65)$$

For the NLO Set-I amplitudes in Eq. (65), the soft divergences from sub-diagrams Figs. 7(h,i) can be canceled by their counterparts from Figs. 7(j,k), then only the collinear divergences are left for the infrared absorbtion. The collinear divergences can all be absorbed into the NLO pion meson DAs of $\phi^{(1),P}_{\pi,d/e}$, which can be written as the nonlocal hadronic matrix element with the structure as that in Ref. [11]:

$$\phi^{(1),P}_{\pi}(x,p_2^2) = \frac{1}{2N_c P_2^-}\int \frac{dy^+}{2\pi} e^{-ixp_2^- y^+} < \pi(p_2)|\overline{q}(y^+)(-ig_s)\int_0^{y^+} dzn\cdot A(zn)\frac{\gamma_5}{2}q(0)|0> . \quad (66)$$

As shown in Eq. (65), all Set-I infrared-relevant NLO amplitudes can be written as the convolution of the LO hard kernel and the NLO π meson DAs ($G^{(0)}_{b,23}\otimes\phi^{(1),P}_{\pi,d}$ and $G^{(0)}_{b,23}\otimes\phi^{(1),P}_{\pi,e}$), with the integral momenta flowing or not flowing into the LO hard amplitudes.

By making the summation for the Set-II amplitudes for the sub-diagrams Figs. 7(d,e,f,g,h,i,j,k) with the T3&T2 DAs, we find:

$$\begin{aligned} G^{(1)}_{7,32}(x_1;x_2) = \phi^{(1),A}_{\pi,d}\otimes\left\{G^{(0)}_{b,32}(x_1;x_2) - G^{(0)}_{b,32}(x_1;\xi_2) + \frac{1}{8}G^{(0)}_{b,32}(x_1;\xi_2,x_2)\right\} \\ +\phi^{(1),A}_{\pi,e}\otimes\left\{G^{(0)}_{b,32}(x_1;x_2) - G^{(0)}_{b,32}(x_1;\xi_2) - \frac{1}{8}G^{''(0)}_{b,32}(x_1;\xi_2,x_2)\right\}. \end{aligned} \quad (67)$$

For the infrared singularities in the Set-II amplitudes in Eq. (67), the soft divergences from Figs. 7(i,j) can't be canceled by their counterparts in Figs. 7(h,k), but these soft divergences are also diminished because $\phi^{(1),A}_{\pi,e} = \phi^{(1),A}_{\pi,d}$. The remaining collinear singularities in Eq. (67) can be absorbed into the NLO DAs $\phi^{(1),A}_{\pi,d/e}$. All these irreducible NLO amplitudes can be written as the convolution of the LO hard kernel and the NLO π meson DAs($G^{(0)}_{b,23}\otimes\phi^{(1),A}_{\pi,e}$ and $G^{(0)}_{b,32}\otimes\phi^{(1),A}_{\pi,e}$), and the collinear factorization approach is valid for the Fig. 7.

III. k_T FACTORIZATION OF $\rho\gamma^\star\to\pi$

In this section, the NLO proof of the factorization theorem is demonstrated with the inclusion of the transversal momentum k_T. The k_T factorization approach is qualified to deal with the small-x physics[2, 6, 9], because of it's advantage to avoid the end-point singularity without introducing other non-physics methods.

The hierarchy $k^2_{iT}\ll k_1\cdot k_2$ is holding in the bound wave functions, so the transversal contributions on the numerators can be dropped safely and the transversal momentum k_T in the LO hard kernels can also be dropped, then factorization proofs made in the above section with the collinear factorization approach is valid here with the inclusion of the transversal momentum [10, 13]. When we extend the proofs for the NLO $\rho\to\pi$ transition from collinear factorization approach to k_T factorization approach, the only modification required is to include the transversal integral l_T to the NLO wave functions in Eqs. (23,24, 46,63,66), besides the longitudinal integral along the light cone. This modification can also be understood as the integral deviated from the light cone direction by $\mathbf{b}$ in the coordinate space, as illustrated by Fig. 8.

The $\mathcal{O}(\alpha_s)$ wave functions at twist-2 and twist-3 as deifined in Eqs. (23,24,46,63,66) can be reproduced by the following nonlocal matrix element in the $\mathbf{b}$ space.

$$\begin{aligned} \phi^{(1),T}_{\rho}(x_1,\xi_1;\mathbf{b_1}) = \frac{1}{2N_c P_1^+}\int\frac{dy^-}{2\pi}\frac{d\mathbf{b_1}}{(2\pi)^2}e^{-ixp_1^+y^+ + i\mathbf{k_{1T}}\cdot\mathbf{b_1}} \\ \cdot <0|\overline{q}(y^-)\frac{\gamma_\perp^b\gamma^+}{4}(-ig_s)\int_0^y dzv\cdot A(zv)q(0)|\rho(p_1)>, \end{aligned} \quad (68)$$

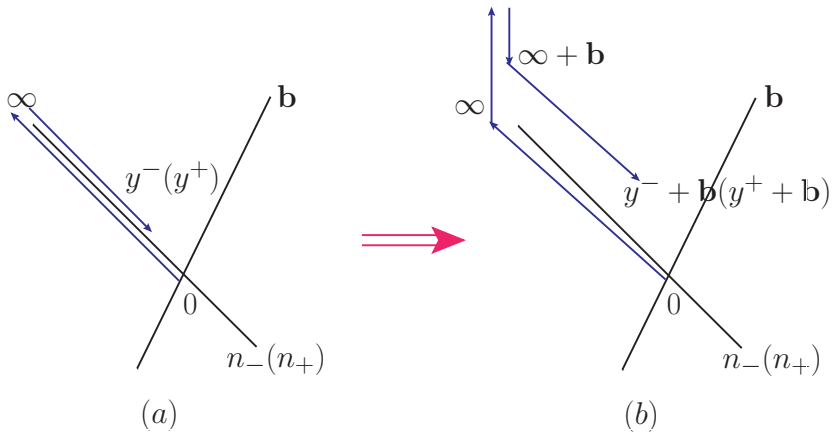

FIG. 8. The deviation of the integral (Wilson link) from the light corn by $\mathbf{b}$ in the coordinate space for the two-parton meson wave function.

$$\phi_\rho^{(1),v}(x_1,\xi_1;\mathbf{b_1}) = \frac{1}{2N_cP_1^+}\int\frac{dy^-}{2\pi}\frac{d\mathbf{b_1}}{(2\pi)^2}e^{-ixp_1^+y^++i\mathbf{k_{1T}}\cdot\mathbf{b_1}} \cdot <0|\overline{q}(y^-)\frac{\gamma_\perp}{2}(-ig_s)\int_0^y dzv\cdot A(zv)q(0)|\rho(p_1)>, \tag{69}$$

$$\phi_\rho^{(1),a}(x_1,\xi_1;\mathbf{b_1}) = \frac{1}{2N_cP_1^+}\int\frac{dy^-}{2\pi}\frac{d\mathbf{b_1}}{(2\pi)^2}e^{-ixp_1^+y^++i\mathbf{k_{1T}}\cdot\mathbf{b_1}} \cdot <0|\overline{q}(y^-)\frac{\gamma_5\gamma_\perp}{2}(-ig_s)\int_0^y dzv\cdot A(zv)q(0)|\rho(p_1)>; \tag{70}$$

$$\phi_\pi^{(1),A}(\xi_2,x_2;\mathbf{b_2}) = \frac{1}{2N_cP_2^-}\int\frac{dy^+}{2\pi}\frac{d\mathbf{b_2}}{(2\pi)^2}e^{-ixp_2^-y^++i\mathbf{k_{2T}}\cdot\mathbf{b_2}} \cdot <\pi(p_2)|\overline{q}(y^+)(-ig_s)\int_0^y dzn\cdot A(zn)\frac{\gamma^-\gamma_5}{2}q(0)|0>, \tag{71}$$

$$\phi_\pi^{(1),P}(\xi_2,x_2;\mathbf{b_2}) = \frac{1}{2N_cP_2^-}\int\frac{dy^+}{2\pi}\frac{d\mathbf{b_2}}{(2\pi)^2}e^{-ixp_2^-y^++i\mathbf{k_{2T}}\cdot\mathbf{b_2}} \cdot <\pi(p_2)|\overline{q}(y^+)(-ig_s)\int_0^y dzn\cdot A(zn)\frac{\gamma_5}{2}q(0)|0>. \tag{72}$$

All these NLO wave functions would reproduce the Feynman rules of Wilson lines.

IV. SUMMAREY

In this paper we firstly verified that the factorization hypothesis is valid for the $\rho\to\pi$ transition process at NLO level in the collinear factorization approach, and then we extended this proof to the case of the k_T factorization approach. Because of the difference of the initial vector meson ρ and the final pseudo-scalar meson π, we considered both the two LO sub-diagrams Figs. 1(a) and

1(b), with the virtual photon vertex positioned on the initial state quark line and on the final state quark line, respectively.

For each LO sub-diagram Fig. 1(a) or Fig. 1(b), we first evaluated the NLO corrections from the additional gluon radiated from the initial rho meson as well as from the final pion meson, and then we verified that all the infrared singularities in those four NLO quark level diagrams (Fig.1(a) - Fig.1(d)) could be absorbed into the NLO meson wave functions. Certainly, we made this proof both in the collinear factorization approach and in the k_T factorization approach. And we showed explicitly that every NLO quark level amplitude can be expressed as the convolution of the NLO wave functions and the LO hard kernel, with the gluon momenta, which would generate the infrared singularities, flowing, not flowing or partly flowing into the LO hard amplitudes.

Particularly, we find that: (a) only the T3&T2 set with the twist-3 ρ meson DAs and twist-2 pion DAs contribute to the LO amplitude of Fig. 1(a), as defined in Eq. (3); (b) only the collinear singularities would appeare in the NLO diagrams for the LO Fig. 1(a), because the soft singularities in these NLO diagrams are either suppressed by the kinetics or canceled each other.

For the NLO corrections to the LO Fig. 1(b), however, there exist two kinds of the LO amplitudes as described in Eqs. (4,5) with the T2&T3 and T3&T2 combinations of the initial and final state meson wave functions and we called them Set-I and Set-II respectively. We further find that the NLO corrections to the Set-I and Set-II LO amplitude generate the collinear singularities only, since the soft singularities in these two cases are either suppressed by the kinetics or canceled each other. The underlying reason is the fact that the soft gluon will not change the color structure of the rho and pion mesons. All the remaining infrared singularities from the collinear regions, should be absorbed into the NLO wave functions, and we have also defined the NLO wave functions with different twists in the nonlocal matrix elements, which would help us to understand the fundamental meson wave functions and push us to calculate the NLO hard kernels for this $\rho \to \pi$ transition process.

V. ACKNOWLEDEMENT

The authors would like to thank H.N. Li and C.D. Lu for long term collaborations and valuable discussions. This work is supported by the National Natural Science Foundation of China under Grant No. 11235005, and by the Project on Graduate Students Education and Innovation of Jiangsu Province, under Grant No. CXZZ13-0391.

[1] John. Collins, Foundations of Perturbative QCD (Cambridge University Press, Cambridge, England, 1993).

[2] G.P. Lepage, and S.J. Brodsky, **Phys. Lett. B 87**, 359(1979); **Phys. Rev. Lett. 43**, 545(1979); **Phys. Rev. D 22**, 2157(1980).

[3] G. Sterman, An introduce to Quantum Field Theory (Cambridge University Press, Cambridge, England, 1993).

[4] M. Beneke, G. Buchalla, M. Neubert, and C.T. Sachrajda, **Phys. Rev. Lett. 83**, 1914 (1999); **Nucl. Phys. B 591**, 313 (2000).

[5] J.C. Collins, and R.K. Ellis, **Nucl. Phys. B 360**, 3 (1991); J. Botts, G. Sterman, **Nucl. Phys. B** 325, 62 (1989); H.N. Li, G. Sterman, **Nucl. Phys. B** 381, 129(1992);

[6] T. Huang, and Q.X. Shen, **Z. Phys. C 50**, 139 (1991).

[7] S. Cantani, M. Ciafaloni, and F. Hautmann, **Nucl. Phys. B 366**, 135 (1991).
[8] P. Ball, V.M. Braun, Y. Koike, and K. Tanaka, **Nucl. Phys. B 529**, 323 (1998).
[9] H.N. Li, **Phys. Rev. D 64**, 014019(2001).
[10] M. Nagashima, and H.N. Li, **Phys. Rev. D 67**, 034001 (2003).
[11] M. Nagashima, and H.N. Li, **Eur. Phys. J. C 40**, 395 (2005).
[12] S. Nandi, and H.N. Li, **Phys. Rev. D 76**, 034008 (2007).
[13] H.N. Li, Y.L. Shen, Y.M. Wang, and H. Zou, **Phys. Rev. D 83**, 054029(2011).
[14] H.N. Li, Y.L. Shen, and Y.M. Wang, **Phys. Rev. D 85**, 074004 (2012).
[15] S. Cheng, Y.Y. Fan, and Z.J. Xiao, **Phys. Rev. D 89**, 054015 (2014).
[16] S. Cheng, Y.Y. Fan, X. Yu, C.D. Lü, and Z.J. Xiao, **Phys. Rev. D 89**, 094004 (2014).
[17] V.V. Braguta, and A.I. Onishchenko, **Phys. Rev. D 70**, 033001 (2004).
[18] J.H. Yu, B.W. Xiao, and B.Q. Ma, **J.Phys.-G- 34**, 1845 (2007).
[19] P. Maris, and P.C. Tendy, **Phys. Rev. C 65**, 045211 (2008).
[20] F. Zuo, Y. Jia, and T. Huang, **Eur. Phys. J. C 67**, 253 (2010)
[21] T. Kurimoto and H.N. Li, **Phys. Rev. D 65**, 014007 (2001).
[22] P. Ball and R, Zwicky, **Phys. Rev. D 71**, 014015(2005).
[23] P. Ball, V.M. Braun and A. Lenz, **J. High Energy Phys. 0605**, 004 (2006). P. Ball, **J. High Energy Phys.** 9809 (1998) 005.
[24] Y.L. Zhang, X.Y. Liu, Y.Y. Fan, S. Cheng, and Z.J. Xiao, **Phys. Rev. D 90**, 014029 (2014).
[25] W. Zinnermann, **Ann. of Phys 77**, 536 (1973).